**Re-evaluating ambiguous age relationships in Archean cratons: implications for the origin of ultramafic-mafic complexes in the Lewisian Gneiss Complex**

George L. Guice[a]*, Iain McDonald[a], Hannah S. R. Hughes[b,c], John M. MacDonald[d], Thomas G. Blenkinsop[a], Kathryn M. Goodenough[e], John W. Faithfull[f], Robert J. Gooday[a]

[a] School of Earth and Ocean Sciences, Cardiff University, Main Building, Park Place, Cardiff, CF10 3AT

[b] Camborne School of Mines, College of Engineering, Mathematics & Physical Sciences, University of Exeter, Penryn Campus, Penryn, Cornwall, TR10 9FE

[c] School of Geosciences, University of the Witwatersrand, Private Bag 3, Wits 2050, Johannesburg South Africa

[d] School of Geographical and Earth Sciences, Gregory Building, University of Glasgow, Glasgow, G12 8QQ

[e] British Geological Survey, Lyell Centre, Research Avenue South, Edinburgh, EH14 4AP

[f] Hunterian Museum, University of Glasgow, University Avenue, Glasgow, G12 8QQ

**Please find revisions marked in red**

*Corresponding author: GuiceG@cardiff.ac.uk

**Keywords:** Archean geodynamics; layered intrusion; ultramafic-mafic complex; North Atlantic Craton; spinel

**ABSTRACT**

Archean ultramafic-mafic complexes have been the focus of important and often contentious geological and geodynamic interpretations. However, their age relative to the other components of Archean cratons are often poorly-constrained, introducing significant ambiguity when interpreting their origin and geodynamic significance. The Lewisian Gneiss Complex (LGC) of the northwest Scottish mainland – a high-grade, tonalite-trondhjemite-granodiorite (TTG) terrane that forms part of the North Atlantic Craton (NAC) – contains a number of ultramafic-mafic complexes whose origin and geodynamic significance have remained enigmatic since they were first described. Previous studies have interpreted these complexes as representing a wide-range of geological environments, from oceanic crust, to the sagducted remnants of Archean greenstone belts. These interpretations, which are often critically dependent upon the ages of the complexes relative to the surrounding rocks, have disparate implications for Archean geodynamic regimes (in the NAC and globally). Most previous authors have inferred that the ultramafic-mafic complexes of the LGC pre-date the TTG magmas. This fundamental age relationship is re-evaluated in this investigation through re-mapping of the Geodh' nan Sgadan Complex (where tonalitic gneiss reportedly cross-cuts mafic rocks) and new mapping of the 7 km$^2$ Ben Strome Complex (the largest ultramafic-mafic complex in the LGC), alongside detailed petrography and spinel mineral chemistry. This new study reveals that, despite their close proximity in the LGC (12 km), the Ben Strome and Geodh' nan Sgadan Complexes are petrogenetically unrelated, indicating that the LGC (and thus NAC) records multiple temporally and/or petrogenetically distinct phases of ultramafic-mafic Archean magmatism that has been masked by subsequent high-grade metamorphism. Moreover, field observations and spinel mineral chemistry demonstrate that the Ben Strome Complex represents a layered intrusion that was emplaced *into* a TTG-dominated crust. Further to representing a significant re-evaluation of the LGC's magmatic evolution, these findings have important implications for the methodologies utilised in deciphering the origin of Archean ultramafic-mafic complexes globally, where material suitable for dating is often unavailable and field relationships are commonly ambiguous.

## 1.0 INTRODUCTION

Archean geodynamic regimes are highly controversial (e.g., Arndt, 2013; Bédard et al., 2013; Kamber, 2015), with some authors arguing that modern-style plate tectonic processes – involving deep subduction, mantle convection and mid-ocean ridges (Stern, 2005, 2008) – predominated (e.g., De Wit et al., 1987, 1992; Polat et al., 2009; Furness et al., 2009, 2015). Others contest that the distinctive rock associations, structures, metamorphic imprints and geochemical signatures of Archean cratons are incompatible with modern-style plate tectonics (e.g., Van Kranendonk et al., 2004; Condie, 2005; Brown, 2008; Bédard et al., 2013; Kamber, 2015; Johnson et al., 2017; Bédard et al., 2018). Alternative interpretations involve the Archean being characterised by a "stagnant-lid" regime that was periodically destabilised by overturns of the crust and/or mantle (e.g., Van Kranendonk et al., 2004; Bédard et al., 2013; Harris and Bédard, 2014; Bédard, 2018). Here we utilise the terms "horizontal tectonics" and "vertical tectonics", in which modern-style plate tectonics represents the former (e.g., De Wit et al., 1992; Furness et al., 2015) and stagnant lid hypothesis represents the latter (e.g., Van Kranendonk et al., 2004; Bédard et al., 2018).

Ultramafic-mafic complexes are volumetrically minor components of Archean cratons, with individual complexes generally occupying less than 100 km$^2$ (Table 1). Despite their size, the range of lithologies present in ultramafic-mafic complexes may be diverse. For example, in the Greenlandic portion of the North Atlantic Craton (NAC), the Seqi Complex is interpreted to contain only intrusive ultramafic rocks (Szilas et al., 2017), while the Fiskenæsset Complex is suggested to comprise a combination of intrusive and extrusive ultramafic and mafic rocks (Table 1; Polat et al., 2009). This variety of lithologies is often further complicated by serpentinisation, alteration and/or polyphase, greenschist- to granulite-facies metamorphism (Table 1). Notwithstanding these complexities, studies of ultramafic-mafic complexes have provided important and often contentious contributions to the Archean geodynamics debate (Table 1), with individual complexes attributed to wide-ranging geological and geodynamic environments, including: Archean ophiolites/fragments of ophiolites that

may represent Archean suture zone(s) (De Wit et al., 1987; Anhaeusser, 2006a); layered intrusions associated with a range of geodynamic environments (Hoatson and Sun, 2002; Ivanic et al., 2010; Wang et al., 2015; Bagas et al., 2016); subduction-related sills emplaced into oceanic crust (Polat et al., 2009); fragments of arc-related oceanic crust (Szilas et al., 2014); the sagducted remnants of greenstone belts (Johnson et al., 2016); and mantle residues following high degrees of partial melting (Szilas et al., 2017). Some interpretations (e.g., the sagduction hypothesis; Johnson et al., 2016) are compatible with vertical tectonics, while others (e.g., the Archean ophiolites hypothesis; Anhaeusser, 2016a) are compatible with horizontal tectonic models for the Archean Earth. A deeper understanding of how different ultramafic-mafic complexes formed and the means to reliably determine whether or not any of them unambiguously represent Archean oceanic crust is central to answering the question of when plate tectonic processes began to operate on Earth.

Much of the debate in this field is a consequence of the inherent difficulty in dating ultramafic-mafic complexes, with their age relative to the other components of Archean cratons often poorly constrained (Whitehouse and Fedo, 2003; Kolb et al., 2013; Szilas et al., 2017). Such problems result from a scarcity or absence of suitable datable minerals (e.g., baddeleyite, zircon), commonly resulting in an overreliance on commonly ambiguous field relationships to decipher relative age relationships (Whitehouse and Fedo, 2003; Ivanic et al., 2010). Further, even if dateable minerals are present, the isotopic system of interest is often so disturbed by subsequent overprinting metamorphic events as to render isochron or regression analysis ambiguous and/or associated with unacceptably large errors (e.g., Timms et al., 2006). Some complexes, such as Zandspruit (Kaapvaal Craton; Table 1), are cross-cut by dateable rocks, providing straightforward field relationships and a quantitative minimum age for the formation of the ultramafic-mafic complex (Anhaeusser, 2015). However, ambiguous field relationships more commonly inhibit confident interpretation of relative ages. For example, the amphibolite-facies Stolzburg layered complex in the Barberton Greenstone Belt (Kaapvaal Craton; Table 1) was originally believed to have been faulted against the host Nelshoogte Schist Belt (Anhaeusser, 1979). Subsequent identification of a chilled contact at the

4

margin of the complex led to a contrasting (and currently accepted) interpretation, whereby it was intrusive into the Nelshoogte Schist Belt (De Wit et al., 1987). The problem of ambiguous age relationships is exacerbated in high-grade cratonic regions, such as the NAC, where the field relationships may be complicated by long-lived, high-temperature metamorphism and partial melting, rather than primary (igneous) processes and relationships (Nutman et al., 2013; Johnson et al., 2016). Such complications are exemplified by the ultramafic-mafic complexes of the Akilia terrane (western Greenland), where detailed field observations by Whitehouse and Fedo (2003) found no evidence to support the original assumption that they pre-date the volumetrically dominant 3.85 – 3.65 Ga tonalitic gneiss.

As a consequence of uncertain age relationships, the origin(s) of the ultramafic-mafic complexes in the Lewisian Gneiss Complex (LGC) – a fragment of the NAC in northwest Scotland – have been ascribed to a wide-range of geological and geodynamic environments, including: one or more layered intrusion(s) (e.g., Bowes et al., 1964); fragments of a pre-TTG, possibly oceanic, mafic-ultramafic crust (e.g., Sills, 1981); accreted oceanic crust (Park and Tarney, 1987); or the sagducted remnants of Archean greenstone belts (Johnson et al., 2016). In this investigation, we present new detailed geological maps, field descriptions, petrography and mineral chemistry for two ultramafic-mafic complexes in the LGC, namely the 7 $km^2$ Ben Strome Complex and 0.2 $km^2$ Geodh' nan Sgadan Complex. Using these data and a critical review of the existing literature, we address the currently enigmatic origin of the ultramafic-mafic complexes, the magmatic evolution of the LGC, and its context within the wider NAC.

## 2.0 REGIONAL GEOLOGY: THE LEWISIAN COMPLEX

The LGC crops out as a 125 km long, 20 km wide coastal strip on the Scottish mainland, partially covered by Neoproterozoic to Ordovician sedimentary successions and located west of the Moine Thrust (Fig. 1; Friend and Kinny, 2001; Park et al., 2002). The LGC predominantly comprises Archean TTG gneiss representing metamorphosed felsic magmatic rocks, with subordinate ultramafic, mafic,

5

and metasedimentary lithologies that are cross-cut by Palaeoproterozoic mafic dykes, with later granitic-pegmatitic sheets in some areas (Peach et al., 1907; Sutton and Watson, 1951; Park, 1970; Wheeler et al., 2010). The mainland LGC was traditionally subdivided into a granulite-facies 'Central Region' bounded by the amphibolite-facies 'Northern' and 'Southern' Regions (Fig. 1). The granulite-facies Central Region is geochemically depleted in Cs, Rb, Th, Ta, U and K (Sheraton et al., 1973), and has been interpreted as representing deeper crustal levels than the amphibolite-facies Northern and Southern Regions, with the mainland LGC representing a faulted but once continuous crustal block (Park and Tarney, 1987). More recently, geochronological studies have led to the suggestion that the LGC comprises a series of terranes that have distinctive protoliths and metamorphic histories (Kinny and Friend, 1997; Friend and Kinny, 2001; Love et al., 2004, 2010; Kinny et al., 2005). Although the number of terranes remains controversial (Park, 2005), the Laxford Shear Zone is generally accepted as representing a significant crustal boundary (Goodenough et al., 2010, 2013). Henceforth, this paper utilises the subdivision of Park and Tarney (1987).

A suite of ultramafic-mafic complexes, including the Camas nam Buth occurrence at Scouriemore (a site of special scientific interest; SSSI), are most commonly exposed in the northern Central Region and occupy areas between 0.3 and 7.0 km$^2$ (Fig. 1; Peach et al., 1907; O'Hara, 1961; Bowes et al., 1964; Davies, 1974; Sills et al., 1982; Rollinson and Gravestock, 2012; Johnson et al., 2012, 2016). The LGC also contains a suite of poorly characterised centimetre- to metre-scale ultramafic-mafic pods that occur throughout both the Central Region and wider LGC (Park, 1991; Park et al., 2002).

### 2.1 Evolution of the Central Region

Numerous studies have attempted to decipher the magmatic and metamorphic history of the Central Region LGC (e.g., Rollinson and Fowler, 1987; Kinny et al., 2005; Whitehouse and Kemp, 2010; Johnson and White, 2011). The following stratigraphic and metamorphic history for the Central Region is generally accepted: (i) intrusion of TTG magmas between 3.0 and 2.8 Ga, forming the precursors to the orthogneiss (Kinny et al., 2005 and references therein); (ii) a granulite-facies

tectonothermal event, known as the 'Badcallian', between 2.8 and 2.7 Ga (Corfu et al., 1994; Crowley et al., 2014); (iii) an amphibolite-facies tectonothermal event, known as the 'Inverian', between 2.5 and 2.4 Ga (Evans, 1965; Beach, 1973; Evans and Lambert, 1974); (iv) intrusion of a Palaeoproterozoic mafic dyke swarm between 2.42 and 2.38 Ga (the 'Scourie Dykes'; Weaver and Tarney, 1981; Heaman and Tarney, 1989; Davies and Heaman, 2014; Hughes et al., 2014); and (v) amphibolite-facies tectonothermal events at ~1.9 and ~1.7 Ga, known collectively as the 'Laxfordian' (Goodenough et al., 2010, 2013).

All of the TTG gneiss in the Central Region experienced the Badcallian metamorphic event, for which peak *P-T* conditions have been estimated at 0.8-1.2 GPa and >900°C (Andersen et al., 1997; Zirkler et al., 2012). This event, which led to widespread partial melting of both TTG gneiss and the mafic portions of the ultramafic-mafic complexes (Johnson et al., 2012, 2013), is characterised by a pervasive, shallow- to moderate-dipping, centimetre-scale gneissosity that exhibits open to isoclinal folds (Wheeler et al., 2010). Partial melting of mafic lithologies manifests as patches and sheets of coarse-grained, plagioclase-rich leucosomes that may contain euhedral clinopyroxene, while partial melting of TTG gneiss manifest as quartz-rich leucosomes (Johnson et al., 2012. 2013).

The Inverian metamorphic event (Evans, 1965) is defined as the localised retrogressive amphibolite-facies metamorphism and deformation that precedes emplacement of the mafic-ultramafic Scourie Dykes, which are steeply-dipping, up to 100 m wide and trend northwest-southeast (Weaver and Tarney, 1981). This event involved the development of localised, northwest-southeast-trending shear zones, but its extent is poorly-constrained due to subsequent re-activation (Park, 1964; Attfield, 1987). The Laxfordian – the amphibolite-facies metamorphism and deformation that post-dates intrusion of the Scourie Dykes (Sutton and Watson, 1951) – encompasses a range of metamorphic and magmatic events (Goodenough et al., 2013) that typically manifests as discrete, broadly east-west-trending shear zones up to tens of metres wide (Goodenough et al., 2013). These shear zones are marked by a steeply-dipping (50-70°) pervasive foliation in the gneisses, thinning of

7

the gneissose layering and tight folding (Kinny et al., 2005; Goodenough et al., 2010, 2013). For comprehensive descriptions of the Laxford Shear Zone, see Goodenough et al. (2010, 2013).

### 2.2 Ultramafic-mafic complexes in the Central Region

Ultramafic-mafic complexes in the Central Region have been reported to contain ultramafic and mafic rocks types in a 1:2 ratio, as observed at Scouriemore (Fig. 1; Bowes et al., 1964; Goodenough and Krabbendam, 2011). However, some complexes, such as Geodh' nan Sgadan and Ben Auskaird, have no ultramafic rocks, while others, such as Lochan Daihm Mor, are almost exclusively ultramafic (Fig. 1). Where both ultramafic and mafic rock types are present, the ultramafic rocks, which often exhibit distinctive primary magmatic layering (Sills, 1981; Sills et al., 1982), commonly form the structural base of complexes (O'Hara, 1961; Johnson et al., 2012). Complexes generally display sheet-like forms and open- to isoclinal Badcallian folds (Davies, 1974), with layering generally concordant to the gneissosity in the underlying and overlying TTG gneiss (Sills, 1981). Some complexes – most prominently in the Laxford Shear Zone – are associated with garnet-biotite, quartzo-feldspathic gneisses that structurally overlie the mafic rocks (Davies, 1974; Cartwright et al., 1985; Johnson et al., 2016). The ultramafic-mafic complexes preserve granulite-facies mineral assemblages, which constrain them to be coeval with or older than the Badcallian metamorphic event (Bowes et al., 1964).

Attempts to constrain the relative age relationships by geochronology have proved inconclusive, with Re-Os dating of the Scouriemore and North Scourie Bay Complexes (Fig. 1; Burton et al., 2000) yielding likely crystallisation dates of 2.68 ± 0.02 Ga and 3.26 Ga ± 0.21 Ga (2σ), while Sm-Nd dating (Whitehouse, 1989) of the Achiltibuie, Drumbeg and Scouriemore Complexes yielded dates of 2.85 Ga ± 0.10 Ga, 2.91 Ga ± 0.06 Ga and 2.67 Ga ± 0.11 Ga (2σ) respectively. U-Pb zircon geochronology from TTG gneisses in northern Central Region yielded similarly disparate results, with a spread of concordant ages from 3.1 to 2.5 Ga (Whitehouse and Kemp, 2010; MacDonald et al., 2015) attributed, in part, to Pb diffusion during the LGC's protracted, high-grade metamorphic evolution

(MacDonald et al., 2013). Despite these disturbances to the U-Pb isotopic system, the protolith crystallisation ages for the TTG gneiss protoliths in the north of the Central Region are generally interpreted as 3.05 – 2.90 Ga (e.g., Kinny and Friend, 1997; MacDonald et al., 2015).

As a consequence of these geochronological ambiguities, the relative age relationships between the ultramafic-mafic complexes and surrounding TTG gneiss have been largely informed by field relationships reported by Rollinson and Windley (1980) at the Geodh' nan Sgadan Complex (Fig. 1; NC 14604170), where tonalitic gneiss was considered to cross-cut the mafic rocks. Although Johnson et al. (2016) found no field evidence (at Geodh' nan Sgadan or elsewhere in the LGC) to support this interpretation, it has been used as evidence for the view that the complexes represent an ultramafic-mafic crust invaded by TTG magmas (Rollinson and Windley, 1980; Park and Tarney, 1987; Park et al., 2002; Rollinson and Gravestock, 2012). Moreover, this interpretation led to the assumption that all ultramafic-mafic rocks in the LGC share a common origin, with all occurrences representing variably sized fragments of a pre-TTG, possibly oceanic, crust (Park and Tarney, 1987; Park et al., 2002). However, Rollinson and Gravestock (2012) questioned this assertion, suggesting that the ultramafic complexes and pods on Scouriemore may be genetically unrelated.

### 3.0 THE BEN STROME COMPLEX

The 7 km$^2$ Ben Strome Complex is located 13 km southeast of Scourie (Fig. 1) and represents the largest ultramafic-mafic complex in the LGC (Fig. 2a). For comparison, the well-studied occurrences at Scouriemore (e.g., Sills, 1981; Sills et al., 1982; Rollinson and Gravestock, 2012), which exhibit many of the salient characteristics of the Ben Strome Complex, collectively cover an area less than 0.5 km$^2$. Despite this, the Ben Strome Complex has been little studied (Josey and Shaw, 1974), with no detailed geological map or comprehensive description of the complex published prior to the research presented in this paper. The Ben Strome Complex is one of the easternmost exposures of the LGC (Fig. 1), bordered by the summit of Ben Strome in the west, Loch an Leathaid Bhuain in the east and the Maldie River in the south (Fig. 2). It is surrounded by and interleaved with TTG gneiss

9

typical of the Central Region LGC and is unconformably overlain by Cambrian quartzite in the east (Fig. 2).

### 3.1 Field relationships

Approximately 70 % of the Ben Strome Complex is composed of mafic rocks predominantly comprising metagabbro, garnet-metagabbro, garnet-amphibolite and amphibolite. The remaining 30 % comprises layered ultramafic rocks (predominantly metapyroxenite, with subordinate metaperidotite) that are most commonly structurally underlain by TTG gneiss and structurally overlain by mafic rocks. However, this association is not ubiquitous, with other associations observed, including: individual packages of ultramafic or mafic rocks surrounded by TTG gneiss (e.g., in the northwest of the complex; Fig. 2a); ultramafic rocks both underlain and overlain by mafic rocks (e.g., in the east of the complex; Fig. 2a). The exposed ultramafic-mafic contacts are gradational (typically over an interval of less than 30 cm) and irregular, with the clearest example occurring in the Maldie River (NC 25843401; Fig. 3a). Although the majority are obscured, the ultramafic-mafic contacts are consistently parallel to the layering in the ultramafic rocks (Fig. 2, Fig. 3b). Contacts between the Ben Strome Complex and surrounding TTG gneiss are sharp and commonly exhibit recrystallised quartz and slickensides, indicating that most are tectonic. On both the outcrop (Fig. 3c) and map scale (Fig. 2a-c), the centimetre-scale TTG gneissosity is concordant to both the layering in the ultramafic rocks and margins of the complex. Consequently, the age-relationship with surrounding TTG gneiss is not clear, with no cross-cutting relationships between TTG gneiss and ultramafic-mafic rocks of the Ben Strome Complex.

An east-west-trending, Laxfordian shear zone divides the Ben Strome Complex into the Leathaid (northern) and Maldie (southern) domains (Fig. 2). The shear zone exhibits a pervasive, millimetre to centimetre-scale foliation and dips of between 50 and 90°, which are generally towards the north (Fig. 2, Fig. 3d, Fig. 4a). Ten to ninety metre-thick, northwest-southeast-trending Scourie Dykes cross-cut both domains of the complex, with one strongly deformed dyke contained entirely with

10

the Laxfordian shear zone (Fig. 2). A northeast-southwest-trending fault is best observed in the Maldie Domain, where it juxtaposes ultramafic and mafic rocks (Fig. 2). The fault is younger than the Ben Strome Complex and cross-cutting Scourie Dykes (Fig. 2), with the limited offset of dykes in the Maldie Domain indicating that they have sub-vertical dips. Occasional centimetre to metre-scale pods of ultramafic and mafic rocks are rare in the surrounding TTG gneiss and show no spatial correlation with the Ben Strome Complex (i.e., their density does not increase with decreasing distance to the edges of the complex).

The numerous packages of layered ultramafic rocks are typically between 5 and 50 m in stratigraphic thickness, persist for hundreds of metres along strike, and form prominent, well-exposed ridges and small crags (Fig. 3b-c,e-f). Generally, these packages are dominated by metapyroxenite (metawebsterite and meta-olivine-websterite), with rare peridotitic (metaharzburgite and/or metalherzolite) layers also present (Fig. 3e-f). Within these ultramafic portions, the contacts between the millimetre- to metre-scale layers of different lithologies are either sharp (Fig. 3e) or gradational, with both contact types present in a ~3 m thick package of ultramafic rocks in the Leathaid Domain (Fig. 3f). Gradational variation in modal mineralogy is also observed within individual layers of metapyroxenite and metaperidotite (Fig. 3f), which rarely are truncated. Ultramafic packages dominated by meta-olivine-websterite commonly exhibit rhythmic, millimetre to centimetre-scale internal layering and sharp contacts with subordinate websterite layers, which are more massive and up to tens of centimetres thick (Fig. 3e). These meta-olivine-websterite-dominated ultramafic packages predominate in the Maldie Domain, with a small number of ultramafic packages that also contain volumetrically significant (>10 vol. %) metaperidotite restricted to the Leathaid Domain (Fig. 2a).

Rather than systematic layering, the mafic portions of the Ben Strome Complex are characterised by sporadic lithological heterogeneity on a scale of centimetres to tens of metres (Fig. 3g-h). Despite this, selected areas, such as the area outlined in Fig. 2b, retain remnants of primary layering that are defined by subtle variations in the modal proportion of plagioclase (Fig. 3h). Within the mafic

11

portions of the complex, higher abundances of garnet-metagabbro (Fig. 3g) commonly exist close to ultramafic-mafic contacts, while plagioclase-rich metagabbro (Fig. 3h) is more common in the northwest of the Leathaid Domain (Fig. 2a). Oxide-rich (magnetite-dominated) horizons are sporadically distributed throughout these portions of the complex, which are cross-cut by plagioclase and pyroxene-rich leucosomes (as identified by Johnson et al., 2012, 2013). These leucosomes occur on a centimetre to metre-scale and generally exhibit irregular morphologies and sharp contacts with the surrounding mafic rocks (Fig. 3i). Rare quartz-rich veins, which likely represent leucosomes formed by partial melting of the surrounding TTG gneiss (c.f. Johnson et al., 2013), also occur in the mafic portions of the complex (Fig. 3j). Such TTG-derived leucosomes are restricted to the peripheries of the complex (typically less than 5 m from TTG-mafic contacts) and are most abundant in the north of the Leathaid Domain.

### 3.2 Structure

The earliest recognised structure in the mapped area is the widespread, regional TTG gneissosity (S1), which comprises millimetre- to centimetre-scale layers of relatively mafic and felsic rocks. Individual layers comprise variable proportions of quartz, plagioclase, pyroxene and hornblende, with minor biotite and orthoclase. The S1 structure is consistently parallel to the layering in the Ben Strome Complex, as shown by outcrop-scale photographs (Fig. 3c), kilometre-scale mapping (Fig. 2c) and structural data (Fig. 4a-d), although it is not clear whether S1 pre- or post-dates the Ben Strome Complex.

Outcrop-scale, tight to isoclinal folds of the S1 structure (F2) in the Leathaid Domain (Fig. 5) reveal east-west to northwest-southeast-trending axial planes that dip moderately to steeply north-northeast and fold hinges that plunge steeply toward the east (Fig. 4d). Isoclinal F2 folds, which have axial planes dipping northwest to northeast, are also recognised on the map-scale, most notably in the west and southeast of the Leathaid Domain (Fig. 2a-c). In the Maldie Domain, the Ben Strome Complex comprises two distinct ultramafic packages separated by a thick package of mafic rocks

(Fig. 2d). These ultramafic units can be distinguished based on their subtly different lithological components, with the upper unit containing a 2 m thick layer of serpentinised metaperidotite not observed in the lower unit. These ultramafic packages are conformable with the overlying/underlying mafic rocks, with no evidence for faulted contacts. Along with the underlying TTG gneisses, the Ben Strome Complex in the Maldie Domain forms an open synform (Fig. 2d). Given the east-west-trending hinge of this kilometre-scale structure (Fig. 4b), it likely correlates with the F2 structures identified in the Leathaid Domain.

As shown by Fig. 2b, S1 and F2 structures are re-folded by an open, north-south-trending structure (F3). The effect of the F3 fold can be observed on the kilometre-scale, where S1 and F2 structures trend northwest-southeast to west-east in the south of the Leathaid Domain (south of the large, central Scourie Dyke; Fig. 2a,c), but trend east-west to northeast-southwest in the north of the Leathaid Domain (Fig. 4e,f). S1, F2 and F3 structures are all cross-cut by (in chronological order): Scourie Dykes, the Laxfordian shear zone and a prominent northeast-southwest-trending fault (Fig. 2a). As these cross-cutting relationships constrain the S1, F2 and F3 structures as older than 2.38 Ga (the lowermost age of Scourie Dyke emplacement in the Central Region LGC; Davies and Heaman, 2014), they can be attributed to the Badcallian and/or Inverian metamorphic events.

### 3.3 Petrography

The majority of sampled ultramafic rocks may be classified as meta-olivine-websterite or metawebsterite, with a small number of metalherzolite, meta-orthopyroxenite and metaharzburgite (Fig. 6). Metaperidotites (Fig. 7a-b) comprise (in modal %): 50–95 % serpentinised olivine, up to 20 % orthopyroxene, up to 30 % clinopyroxene, up to 10 % amphibole and up to 5 % spinel. Serpentine is almost ubiquitous in its replacement of olivine, with small (less than 0.5 mm diameter) olivine remnants preserved within large, millimetre to centimetre-scale, serpentine pseudomorphs (Fig. 7a-b). These areas of serpentinisation also contain fine-grained (less than 0.1 mm diameter) magnetite. Pyroxene is 0.7 to 1.6 mm in diameter and subhedral to anhedral, with ortho- and clino-pyroxene

generally occurring in equal proportions. The degree of replacement of clinopyroxene by fine-grained (up to 0.3 mm diameter) amphibole varies between samples. Pargasite (see supplementary material for chemical analyses), which exhibits green-brown pleochroism and 120° triple junctions, is up to 2 mm in diameter. Subhedral to anhedral spinel is 0.2 to 1.2 mm in diameter, while Fe-Ni-Cu sulphides occur as anhedral to subhedral up to 0.15 mm in diameter.

Metapyroxenites (Fig. 7c-f) comprise (in modal %): 25-90 % orthopyroxene, 3–65 % clinopyroxene, up to 40 % serpentinised olivine, up to 45 % pargasite and up to 7 % spinel. A small number of thin sections exhibit the gradational variation in modal mineral proportions described within individual layers on the outcrop-scale (section 3.1), with serpentinised olivine contents grading from less than 5 % to more than 35 % over a 3 cm long thin section. Pyroxene is 0.3 to 3 mm in diameter and exhibits anhedral, subhedral and euhedral forms, with orthopyroxene – the only ubiquitous silicate phase – commonly dominant over clinopyroxene (Fig. 7c-f). Larger pyroxene grains, which are typically between 1.0 and 1.6 mm in diameter, are commonly anhedral to subhedral. By contrast, smaller pyroxene, which is typically less than 0.8 mm in diameter, are commonly subhedral and exhibit 120° triple junctions (Fig. 7d). Pargasite (see supplementary material for chemical analyses), which is up to 4 mm in diameter, exhibits green-brown pleochroism and 120° triple junctions. Olivine in the Leathaid Domain is almost entirely replaced by serpentine, but unserpentinised olivine remnants may constitute up to 5 modal % in the Maldie Domain. Spinel is less than 2 mm in diameter and subhedral to anhedral, while sulphides are anhedral to subhedral and up to 0.12 mm in diameter.

Mafic rocks (Fig. 7g-h), including metagabbro garnet-metagabbro, garnet-amphibolite and amphibolite, comprise (in modal %): 5-70 % clinopyroxene, 15-60 % amphibole, up to 30 % plagioclase, up to 40 % garnet, up to 10 % orthopyroxene and up to 10 % quartz, with accessory ilmenite, spinel, magnetite and sulphides also present. There is significant variation in the modal mineral percentages across the range of mafic rocks, with clinopyroxene and amphibole the only ubiquitous silicate phases (Fig. 7g-h). Moreover, the mafic rocks exhibit a large degree of textural

14

variability. Clinopyroxene are commonly subhedral, range from 0.5 to 2.0 mm in diameter and show varying degrees of retrograde metamorphism to amphibole. This green-brown, pleochroic amphibole ranges from 0.5 to 1.0 mm in diameter and commonly displays evidence for textural equilibrium. Finer-grained (less than 0.3 mm diameter), subhedral amphibole co-exists with similarly-sized plagioclase, forming centimetre-scale interstitial patches that are intergrown with subhedral to anhedral quartz up to 0.1 mm in diameter (Fig. 7h). Plagioclase is most commonly 0.4 to 0.9 mm in diameter and subhedral. Millimetre- to centimetre-scale, anhedral to subhedral garnet porphyroblasts are commonly surrounded by retrogressive plagioclase rims and may also be overgrown by fine-grained clinopyroxene and/or amphibole (Fig. 7g). Anhedral magnetite is the dominant oxide phase and is less than 0.3 mm in diameter. Rare ilmenite is anhedral and up to 0.7 mm in diameter, while fine-grained sulphides (less than 0.2 mm in diameter) are typically anhedral and associated with the boundaries between silicate minerals.

### 3.4 Spinel Mineral Chemistry

Spinels are routinely used as petrogenetic indicators due to their occurrence in a variety of magmatic, tectonic and metamorphic environments (Barnes and Roeder, 2001). Their suitability for these studies is enhanced by the wide-range of conditions at which they crystallise (in ultramafic and mafic magmas) and resistance to alteration relative to other high-temperature minerals (e.g., olivine; Barnes and Roeder, 2001). The ultramafic rocks of the Ben Strome Complex contain both primary and secondary spinel, with primary spinels occurring as euhedral to subhedral, up to 2 mm diameter grains that comprise up to 3 modal % of samples (Fig. 8). These pale- to dark-green (in ppl) grains, which experienced the polyphase high-grade metamorphism outlined above (up to granulite-facies), are most abundant in metapyroxenite samples (Fig. 7c-f; Fig. 8). Secondary spinels, which are the product of serpentinisation and are therefore abundant in serpentine-rich samples, occur as generally elongate, anhedral and opaque (in ppl and xpl) grains up to 0.8 mm in length. In order to assess the petrogenetic environment of the Ben Strome Complex, 314 analyses were conducted on the cores of primary spinel grains from 7 metapyroxenite samples. Two samples were collected from

15

the well-exposed package of ultramafic rocks in the north of the Maldie Domain, with 5 samples collected from the Leathaid Domain (see Fig. 2a and the supplementary material for sample locations). Four of the samples from the Leathaid Domain were collected from the outstanding exposure detailed in Fig. 3f.

Quantitative mineral analyses were carried out using a Zeiss Sigma HD Field Emission Gun Analytical Scanning Electron Microscope (A-SEM) equipped with two Oxford Instruments 150 $mm^2$ EDS detectors, at Cardiff University. Operating conditions were set at 20kV, with analytical drift checks carried out every 20 minutes using a Co reference standard. Suites of standards from ASTIMIX and Smithsonian were used to calibrate the EDS analyser and perform regular secondary standard checks every hour. The raw data were recalculated to element oxides percentages, with $Fe^{2+}$ and $Fe^{3+}$ calculated using the stoichiometric method of Droop (1987). Representative analyses can be found in Table 2 and all the data are available in the supplementary dataset.

The chemistry of Ben Strome spinel has been assessed according to the key compositional parameters outlined by Barnes and Roeder (2001) and Warren (2016). Figure 9 compares the composition of Ben Strome spinels to those from layered intrusions, ophiolites and komatiites, alongside amphibolite-facies magnetite rims and those that nucleated during high-grade metamorphism. As with the Ben Strome spinels, which may have had their compositions altered slightly during high-grade metamorphism, the layered intrusion, ophiolite and komatiite fields of Barnes and Roeder (2001) contains spinels that have experienced metamorphism (of varying styles and grades). The Cr# (calculated as molar Cr/(Cr+Al) x 100) of Ben Strome spinel range from 66.7 to 87.3, with Mg# (calculated as molar Mg/(Mg+$Fe^{2+}$+$Fe^{3+}$) x 100) ranging from 0.8 to 3.4. The $Fe^{2+}$# (calculated as molar $Fe^{2+}$/($Fe^{2+}$+Mg)) of Ben Strome spinel ranges from 0.9 to 1.0, the $Fe^{3+}$# (calculated as molar $Fe^{3+}$/(Cr+Al+$Fe^{3+}$)) ranges from 0.8 to 1.0 and all the $TiO_2$ contents are less than 2.2 wt. % (Fig. 9; Table 2).

The Ben Strome spinels are magnetites that show considerable overlap with the magnetite portions of the layered intrusion field on all plots detailed in Figure 9 (Barnes and Roeder, 2001). By contrast, Ben Strome spinels are compositionally distinct from the ophiolites field (Barnes and Roeder, 2001) on the $Fe^{2+}\#$ versus $Fe^{3+}\#$ plot, $Fe^{3+}\#$ versus $TiO_2$ plot and $Fe^{3+}\#$ - Cr – Al ternary plot, although there is minor overlap with this field on the $Fe^{2+}\#$ versus Cr# plot (Fig. 9). Ben Strome spinels are compositionally distinct from the komatiite field on the $Fe^{2+}\#$ versus $Fe^{3+}\#$ plot, $Fe^{3+}\#$ versus $TiO_2$ plot and $Fe^{3+}\#$ - Cr - Al ternary plot, although there is significant overlap on the $Fe^{2+}\#$ versus Cr# plot (Fig. 9). They are compositionally distinct from the high-grade metamorphic spinel field (Barnes and Roeder, 2001) on $Fe^{2+}\#$ versus $Fe^{3+}\#$ plot and $Fe^{3+}\#$ - Cr - Al ternary plot, although there is significant overlap on the $Fe^{2+}$ versus Cr# plot (Fig. 9). Finally, Ben Strome spinel compositions are distinct from the amphibolite-facies magnetite rims field (Barnes and Roeder, 2001) on the $Fe^{2+}\#$ versus Cr# plot and $Fe^{3+}\#$ - Cr - Al ternary plot, with significant overlap on the $Fe^{2+}\#$ versus $Fe^{3+}\#$ plot (Fig. 9).

## 4.0 THE GEODH' NAN SGADAN COMPLEX

The 0.2 km$^2$ Geodh' nan Sgadan Complex represents the only reported occurrence of TTG gneiss cross-cutting mafic rocks in the LGC (Fig. 10). Given its importance in informing the regional age relationships, this locality was re-mapped (Fig. 10a). Located 15 km northwest of Ben Strome and ~ 1 km ESE of Badcall, Geodh' nan Sgadan is also located in the north of the Central Region (Fig. 1).

### 4.1 Field relationships

The Geodh' nan Sgadan Complex (Fig. 10a; Fig. 11) comprises a ~15 m thick package of layered mafic rocks structurally overlain and underlain by TTG gneiss. Layered ultramafic rocks like those observed in the Ben Strome Complex are notably absent (Fig. 10a). TTG gneiss exhibits a well-defined gneissosity that is locally folded and contains centimetre to metre-scale pods of mafic and ultramafic rocks (Fig. 11a), which show elongation parallel to the gneissosity. Contacts between TTG gneiss and mafic rocks are sharp, with the layering in the mafic rocks parallel to TTG gneissosity (Fig. 10a). Both layering and gneissosity generally strike north-south to northeast-southwest and dip between 26

and 38° towards the west-northwest (Fig. 10a). In the south of the mapped area, both felsic and mafic rocks are folded into northwest-southeast-striking orientations, where both units are truncated by a northeast-southwest-striking brittle fault (Fig. 10a; Fig. 11b).

Layering in the mafic rocks at Geodh' nan Sgadan is highlighted by a millimetre-scale variation in feldspar modal percentages and rare centimetre-scale layers of metapyroxenite (Fig. 11c). Relative to the Ben Strome Complex, mafic rocks are plagioclase-rich, with garnet-metagabbro restricted to rare, metre-scale horizons within metagabbro (Fig. 11d). Layering ranges from well-defined and laterally continuous to poorly-defined and chaotic, with common truncation of layers (Fig. 10e). Mafic rocks are extensively cross-cut by discordant felsic leucosomes (as identified by Johnson et al., 2013) that contain characteristic blue quartz and range from millimetre- to metre-scale (Fig. 10a-b; Fig. 11f-g). A metre-scale, layering-parallel sheet of massive trondhjemite is located towards the stratigraphic top of the package of mafic rocks (Fig. 10b; Fig. 11h).

### 4.2 Comparison to the previously published map

The map and associated log presented in this study (Fig. 10a-b) display some key differences to the map published by Rollinson and Windley (1980; Fig. 10c). Although minor differences result from respective mapping styles, it is necessary to here clarify the major differences. First, Rollinson and Windley (1980; Fig. 10c) subdivided the mafic rocks into separate leucogabbro and gabbro units, whereas the map presented here groups all of these rocks into a unit of "gabbro-dominated mafic rocks" (Fig. 10a-b). We recognise the significant lithological variability within this unit, but identified no systematic spatial variability and therefore elected to represent the lithological variation in log form (Fig. 10b). Second, the map presented in this study identifies a northeast-southwest-trending fault that truncates both the layering in the mafic rocks and gneissosity in the TTG gneiss (Fig. 10a). The presence of this fault, which exhibits a strike consistent with regional faulting patterns (BGS, 2011), is not shown by the map of Rollinson and Windley (1980; Fig. 10c), who reported that "layering in the gabbro is truncated by tonalitic gneiss indicating that the gabbro complexes…are

18

older that the tonalitic gneisses". Third, the intrusive trondhjemite recorded by Rollinson and Windley (1980; Fig. 10c) is represented on the log presented in this study (Fig. 10b), instead of the map, as a result of it occupying less than 1 m in plan view and exhibiting variable thickness. (Fig. 10a). Finally, the scale of the log presented in this study (Fig. 10b) allows us to include cross-cutting quartz-feldspar pegmatites omitted from the maps published both here and by Rollinson and Windley (1980).

### 4.3 Petrography

Although the samples exhibit a small degree of textural variability, all samples can be broadly classified as metagabbro (Fig. 12). Samples comprise (in modal %): 15-60 % amphibole, up to 75 % feldspar, up to 20 % clinopyroxene and up to 5 % orthopyroxene, with rare <0.3 mm diameter sulphides. It should also be noted that rare orthpyroxene-rich layers are present, but were not sampled. Clinopyroxene generally occurs as 0.2 to 0.6 mm diameter, subhedral to euhedral grains that exhibit some alteration to fine-grained amphibole (Fig. 12), with such alteration commonly forming thick (< 0.1 mm) rims (Fig. 12a). Amphibole also occur as subhedral grains that exhibit 120° triple junctions and range from 0.2 to 0.5 mm in diameter (Fig. 12a-b). Feldspar (dominantly plagioclase, with subordinate alkali-feldspar) are generally subhedral and 0.4 to 0.6 mm in diameter, with occasional triple junctions and variable replacement by amphibole (Fig. 12). Orthopyroxene is generally subhedral and less than 0.3 mm in diameter (Fig. 12d). These plagioclase, orthopyroxene and clinopyroxene grains are surrounded by a fine-grained groundmass of amphibole (Fig. 12).

## 5.0 DISCUSSION

### 5.1 Ben Strome and Geodh' nan Sgadan: evidence for multiple ultramafic-mafic suites in the LGC?

The Ben Strome Complex shares many of its salient features with ultramafic-mafic complexes described elsewhere in the LGC, such as those at Scouriemore, Drumbeg and Achiltibuie (Fig. 1; e.g., O'Hara, 1961; Bowes et al., 1964; Sills, 1981; Sills et al., 1982; Johnson et al., 2012):

1. Ultramafic and mafic rocks occur in a roughly 1:2 ratio, with the ultramafic portions generally found at the structural base of the complex, although this association is not ubiquitous (Fig. 2; O'Hara, 1961; Bowes et al., 1964; Sills et al., 1982; Goodenough and Krabbendam, 2011; Johnson et al., 2012, 2016).

2. The ultramafic portions of the complex exhibit distinctive millimetre to metre-scale layering with distinctive (often gradational) changes in modal silicate mineralogy and lithology. This layering, which, despite experiencing high-grade metamorphism, is very similar to that observed in layered intrusions globally, is laterally continuous across entire ultramafic packages (Fig. 2; Fig. 3; Bowes et al., 1964; Sills, 1981; Sills et al., 1982; Johnson et al., 2012).

3. The mafic portions of the Ben Strome Complex are heterogeneous, garnet and clinopyroxene-rich, and exhibit garnet retrogression to plagioclase and orthopyroxene (± hornblende and magnetite; Sills, 1981; Johnson and White, 2011).

4. Despite being tightly folded (along with the adjacent TTG gneiss; Fig. 5; Bowes et al., 1964), magmatic layering in the Ben Strome Complex is consistently parallel with both the TTG gneissosity and margins of the complex (Fig. 2; Bowes et al., 1964; Sills, 1981; Johnson et al., 2012, 2016). There is consistent parallelism between the TTG gneissosity, and magmatic layering in the ultramafic portions of the Ben Strome Complex. The presence of slickensides and, in some cases, recrystallised quartz at ultramafic-TTG gneiss contacts, indicate that these ultramafic slivers experienced polyphase shearing along the contacts of the Ben Strome Complex.

We consider the Ben Strome Complex to represent the largest (by an order of magnitude) example of a layered ultramafic-mafic complex in the Central Region LGC, displaying salient features directly comparable to the exposures at Scouriemore, Drumbeg and Achiltibuie (e.g., Sills, 1981; Sills et al., 1982; Rollinson and Gravestock, 2012). Given its larger size and excellent exposure, the Ben Strome Complex provides crucial evidence pertaining to the genesis of such layered ultramafic-mafic complexes.

20

By contrast, the Geodh' nan Sgadan Complex represents a small occurrence of mafic rocks in the LGC that displays a number of characteristics notably distinct from those reported for the Ben Strome Complex:

1. Geodh' nan Sgadan does not contain the distinctly layered ultramafic rocks that characterise the ultramafic-mafic complexes at Ben Strome, Scouriemore, Achiltibuie and Drumbeg (this study; Sills, 1981; Rollinson and Gravestock, 2012).

2. The mafic rocks consistently exhibit prominent millimetre-scale layering defined by variation in plagioclase modal percentages (Fig. 11) that is not recorded at other ultramafic-mafic complexes in the LGC.

3. The garnet-rich mafic rocks that characterise the Ben Strome, Scouriemore, Drumbeg and Achiltibuie Complexes are restricted to rare, centimetre-scale horizons at Geodh' nan Sgadan (this study; Sills, 1981).

4. The mafic rocks at Geodh' nan Sgadan are comparatively plagioclase-rich (up to 75 modal %) and fine-grained, with clinopyroxene and plagioclase typically 200 to 400 μm in diameter. By contrast, plagioclase always comprises less than 30 modal % of mafic rocks at Ben Strome and clinopyroxene/plagioclase crystals range from 0.4 to 2.0 mm diameter. Moreover, alkali-feldspar occurs rarely at Geodh' nan Sgadan, but is completely absent in the Ben Strome mafic rocks.

Further to being truncated by multiple Scourie Dykes, the Geodh' nan Sgadan Complex displays multiple features characteristic of the Badcallian metamorphic event, including: a moderate-dipping gneissosity in the TTG gneisses surrounding the complex; granoblastic textures within the mafic rocks; and the presence of quartz-feldspar pegmatite (derived from partial melting; Johnson et al., 2013). The Geodh' nan Sgadan Complex therefore experienced the same broad metamorphic history as the Ben Strome Complex (section 3.2), with the contrasting features outlined above considered to be predominantly the result of primary processes. Although these differences may be explained by faulting exposing different stratigraphic levels in one ultramafic-mafic sequence (as proposed by

21

Johnson et al., 2016), there exists the possibility that there may be more than one suite of ultramafic-mafic complexes in the LGC, as initially proposed by Rollinson and Gravestock (2012). The Geodh' nan Sgadan Complex may be petrogenetically unrelated to some of the other ultramafic-mafic complexes in the LGC, where layered ultramafic rocks are characteristically accompanied by garnet-rich mafic rocks (e.g., Ben Strome, Scouriemore, Drumbeg and Achiltibuie). Our field observations add to growing evidence (including the mineral chemistry of Rollinson and Gravestock, 2012) for a scenario whereby the LGC records more than one phase of Archean mafic and/or ultramafic-mafic magmatism prior to the Badcallian metamorphic event. This underlines the possibility that high-grade metamorphic events, such as the Badcallian in the LGC, may obscure temporally and/or petrogenetically distinct magmatic events, as may be typical in marginal cratonic regions (such as the LGC, within the wider NAC). This supports the study of Kolb et al. (2015), who identified multiple episodes of Archean ultramafic-mafic magmatism in the Greenlandic portion of the NAC.

### 5.2 Origin of ultramafic-mafic complexes in the LGC

#### *5.2.1 Layered ultramafic-mafic complexes*

The observations reported in this study reveal that the Ben Strome Complex exhibits a range of features that are consistent with and characteristic of layered intrusions (Namur et al., 2015), such as: (i) laterally continuous igneous layering (Fig. 3a-c, e-f); (ii) gradational contacts between ultramafic and mafic units (Fig. 3a); (iii) gradational contacts between centimetre to metre-scale metaperidotite and metapyroxenite layers (Fig. 3f); (iv) existence of multiple ultramafic units within one continuous stratigraphic sequence (e.g., in the Maldie Domain; Fig. 2a,d), which may represent multiple megacyclic units; (v) occasional truncation of layers within ultramafic units; and (vi) gradational variation in mineral composition within individual ultramafic layers on a scale of tens of centimetres. These field observations are consistent with the composition of spinel, which consistently correspond with the layered intrusion field (Fig. 9). By contrast, spinel compositions are

distinct from both the komatiite and ophiolite/oceanic peridotite fields (Fig. 9). These data contradict the accreted oceanic crust hypothesis for the genesis of such ultramafic-mafic complexes in the LGC of Park and Tarney (1987). Johnson et al. (2016) invoked the sagduction hypothesis (whereby remnants of greenstone belts sank into partially molten TTG) to explain the spatial association between brown gneisses, which may represent metasedimentary rocks, and some of the layered ultramafic-mafic complexes (notably in the Laxford Shear Zone). The composition of spinel and distinct absence of metasedimentary rocks or demonstrably metamorphosed extrusive units (common components of Archean greenstone belts (e.g., Brandl et al., 2006)) within the Ben Strome Complex is contrary to this interpretation. Consequently, we consider our paradigm, whereby the Ben Strome Complex (and associated layered ultramafic-mafic complexes in the LGC; e.g., Achiltibuie and Drumbeg) represents a layered intrusion, to be more compatible with the data presented here.

Identification of the Ben Strome Complex as a layered intrusion does not, however, solve the crucial age relationship quandary. Was the Ben Strome Complex emplaced into an early mafic-ultramafic crust that was subsequently invaded by TTG magmas – a model similar to the pre-TTG mafic-ultramafic crust hypothesis of Sills (1981) – or, alternatively, was it emplaced into TTG gneiss protoliths? Although the Ben Strome Complex demonstrably pre-dates the Badcallian metamorphic event (section 3.2), it is unclear whether the intrusion pre- or post-dates the development of the S1 gneissosity. One speculative possibility, which satisfies the consistent parallelism between S1 gneissosity and magmatic layering in the Ben Strome Complex, is that the S1 gneissosity was developed prior to the intrusion of Ben Strome. In this scenario, the S1 gneissosity may have facilitated the emplacement of the Ben Strome Complex as a sill-shaped intrusion in a manner similar to bedding-parallel sills. Alternatively, the rheology contrast between the ultramafic-mafic rocks of the Ben Strome Complex and surrounding TTG gneiss could have facilitated S1 development in the latter, but not the former. This could also have generated the consistent parallelism between the S1 gneissosity and magmatic layering, regardless of the relative age relationship.

Sills (1981) argued that the seemingly chaotic distribution of the ultramafic-mafic complexes amongst the TTG gneiss is evidence for the pre-TTG mafic-ultramafic crust model. Such a distribution is evident in the west of the Leathaid Domain at Ben Strome, where slivers of ultramafic and mafic rocks are surrounded by TTG gneiss (Fig. 2a). In this area, individual slivers are up to 40 m thick, extend for up to 750 m along strike and occasionally exhibit tight F2 folds. However, this distribution may also be explained by polyphase shearing along lithological contacts, which is an interpretation supported by the observed field evidence involving slickensides and recrystallised quartz at exposed contacts between ultramafic rocks and TTG gneiss. Based on the F2 folding of ultramafic slivers in the northwest of the Ben Strome Complex (Fig. 2), such shearing – if indeed responsible for the observed outcrop patterns – must have initially preceded the major folding events that affected the Ben Strome Complex, with the subsequent reactivation during the LGC's protracted and polyphase metamorphic history responsible for the preservation of slickensides.

If the Ben Strome Complex was not emplaced into TTG gneiss, what did it intrude and where is that material now? This question represents the biggest conceptual predicament associated with any interpretation that requires that the Ben Strome Complex preceded the TTG magmas. In the Johannesburg Dome, the Zandspruit ultramafic-mafic complex – an Archean layered intrusion that was emplaced into a greenstone belt and subsequently invaded by TTG magmas – preserves evidence of the metavolcanic rocks that it intruded, despite the exposed intrusion and intruded greenstone belt covering a combined area of less than 1 $km^2$ (Anhaeusser, 2015). Similarly, the granulite-facies Fiskenæsset Complex (Greenland, NAC), which comprises a series of arc-related, intrusive sills, preserves evidence for the extrusive units intruded by those sills (Polat et al., 2009). By contrast, the Ben Strome Complex and surrounding TTG gneiss preserve no evidence for any material that the magmas could have conceivably been emplaced into (other than the surrounding TTG gneiss). The small ultramafic-mafic pods that are distributed throughout the LGC represent the obvious candidates, but these pods are exceptionally rare in the TTG gneiss surrounding the Ben Strome Complex. By contrast, granulite-facies ultramafic-mafic complexes that have been

24

unambiguously invaded by TTG magmas in the Greenlandic portion of the NAC, namely Seqi and Fiskenæsset, exhibit a high concentration of ultramafic-mafic pods at their margins (Polat et al., 2009; Bagas et al., 2016; Szilas et al., 2017). At Seqi, these pods occur as elongate lenses of amphibolite that are up to 40 m long and 25 m wide (Szilas et al., 2017). Consequently, we consider it extremely unlikely that the rare ultramafic-mafic pods found in TTG gneiss throughout the Central Region of the LGC represent small fragments of crust that the Ben Strome Complex intruded prior to being invaded by TTG magmas.

In summary, given the absence of unambiguous evidence supporting the interpretation whereby the Ben Strome Complex predates the surrounding TTG gneiss, we propose a simple model, whereby the Complex was emplaced *into* the TTG gneiss that constitutes the bulk of the LGC.

### 5.2.2 Non-layered complexes

In contrast to the Ben Strome Complex, the origin of the Geodh' nan Sgadan Complex remains harder to establish. The presence (albeit at a low abundance) of alkali-feldspar and high modal percentages of plagioclase in the Geodh' nan Sgadan rocks indicate that this occurrence crystallised from more felsic magmas than those of the Ben Strome Complex. However, the lack of primary spinel within these rocks prevents any quantitative petrogenetic comparison to the Ben Strome Complex. The previously reported, map-scale crossing cutting relationship of Rollinson and Windley (1980) is challenged by the evidence for a tectonic contact identified in this study (Fig. 10a; Fig. 11b) and it remains uncertain whether the complex pre- or post-dates the TTG magmas. This age relationship hinges on the genetic association between the trondhjemite sheets and surrounding TTG gneiss. Are these sheets, which intrude into the Geodh' nan Sgadan Complex (as originally suggested by Rollinson and Windley, 1980), associated with the initial emplacement of the TTG magmas or, alternatively, are they the product of Badcallian partial melting? While our field descriptions of the trondhjemite sheets hint at a partial melting origin (Johnson et al,. 2013), the relatively high concentration of mafic pods located close to the margin of the complex may hint that

25

these mafic rocks were invaded and fragmented by the TTG gneiss protoliths. In summary, in the case of Geodh' nan Sgadan, it is not possible to definitively comment on whether these mafic rocks pre- or post-date the TTG gneiss and consequently, the petrogenesis of this small complex remains enigmatic.

### 5.2.3   Wider context and future work

Largely as a consequence of uncertain age relationships, which commonly introduces significant ambiguity to Archean geodynamic interpretations (see Section 1.0), the ultramafic-mafic complexes of the LGC have been subject to wide-ranging interpretations. As detailed in Figure 13, these hypotheses have disparate implications for interpretations of Archean geodynamic regime(s), both in the wider NAC and Archean cratons globally. The sagduction hypothesis of Johnson et al. (2016), which involves fragments of Archean greenstone belts sinking into partially molten TTG (Fig. 13), supports the vertical tectonics view of the Archean Earth. By contrast, the accreted oceanic crust hypothesis of Park and Tarney (1987), which envisages the complexes as representing oceanic crust that was obducted during modern-style subduction processes (Fig. 13), supports the horizontal tectonics view of the Archean Earth. The interpretation proposed in this study – whereby the layered ultramafic-mafic complexes in the LGC represent deformed layered intrusions (see Section 5.2.1) – may be applicable to a number of geodynamic environments (Fig. 13). Some of these environments are specific to horizontal tectonics (e.g., subduction and mid-ocean-related magmatism), while others can be applied to both horizontal and vertical tectonics (e.g., plume-related magmatism; Fig. 13). The present study of the Ben Strome Complex highlights how identification of relative age relationships can greatly enhance interpretations of ultramafic-mafic complexes in Archean cratons. This is reinforced by the study of the Geodh' nan Sgadan Complex, where relative age relationships remain unclear and, consequently, the geological and geodynamic environments within which it formed remains enigmatic. Thus, only by a rigorous field campaign, through structural understanding and petrographic investigation may future geochemical studies be successful in

investigating the geodynamic environments within which ultramafic-mafic complexes formed. Such studies may reveal the extent to which interpretations from the Ben Strome Complex can be extended to other ultramafic-mafic complexes in the LGC and wider NAC. Indeed, a thorough debate on the timing of the formation of such complexes, on a case-by-case basis, is crucial in order to apply geochemistry meaningfully to high-grade cratonic regions.

## CONCLUSIONS

1. As a result of ambiguous field relationships and a scarcity of minerals suitable for geochronology, ultramafic-mafic complexes in Archean cratons commonly exhibit unclear relative age relationships with the surrounding rocks. As a consequence, interpretations of ultramafic-mafic complexes are diverse and have disparate implications for Archean geodynamic regimes. By applying an Ockham's Razor approach to the previously unstudied Ben Strome Complex, which represents the largest ultramafic-mafic complex in the LGC, it is concluded that it represents a layered intrusion emplaced *into* the surrounding TTG gneiss. Conversely, the origin of the Geodh' nan Sgadan Complex remains enigmatic as a consequence of its unclear age relationships with surrounding TTG gneiss.

2. The Ben Strome Complex shares salient features with the ultramafic-mafic complexes at Scouriemore, Drumbeg and Achiltibuie, which may represent genetically-related layered intrusions that were also emplaced into the TTG gneiss. This interpretation represents a significant re-evaluation of the magmatic evolution of the LGC, but is not specific to any particular geodynamic regime (e.g., horizontal or vertical tectonics) having operated during the Archean.

3. High-grade metamorphic processes may mask temporally/ petrogenetically distinct phases of crustal growth recorded by suites of ultramafic-mafic complexes in Archean cratons. Rather than all ultramafic-mafic complexes in cratons representing singular events, it is highly likely that the portions of Archean crust, such as that represented by the LGC,

27

experienced multiple phases of ultramafic and/or mafic magmatism during the Meso- and Neo-Archean – geological eras that, combined, span 700 Ma. In the LGC, this is exemplified by the disparate salient features of the Ben Strome and Geodh' nan Sgadan Complexes, which we here consider to be petrogenetically unrelated.

## ACKNOWLEDGEMENTS AND FUNDING

## APPENDICES

Supplementary material A: spinel mineral chemistry.

Supplementary material B: sample locations.

Supplementary material C: amphibole mineral chemistry.

**REFERENCES**

Andersen, T., Whitehouse, M. J., Burke, E. A. J. 1997. Fluid inclusions in Scourian granulites from the Lewisian complex of NW Scotland: evidence for CO2-rich fluid in Late Archean high-grade metamorphism. *Lithos*, **40**, 93-104.

Anhaeusser, C. R. 1979. Rodingite occurrences in some Archean ultramafic complexes in the Barberton Mountain Land, South Africa. *Precambrian Research*, **8**, 49-76.

Anhaeusser, C. R. 2001. The anatomy of an extrusive-intrusive Archean mafic-ultramafic sequence: the Nelshoogte Schist Belt and Stolzburg Layered Ultramafic Complex, Barberton Greenstone Belt, South Africa. *South African Journal of Geology.* **104,** 167-204.

Anhaeusser, C. R. 2006a. A re-evaluation of Archean intracratonic terrane boundaries on the Kaapvaal Craton, South Africa: Collisional suture zones? *Geol. Soc. Am. Spec. Pap.* **405,** 193-210.

Anhaeusser, C. R. 2006b. Ultramafic and mafic intrusion of the Kaapvaal Craton. *Geology of South Africa.* 95-134.

Anhaeusser, C. R. 2015. Metasomatized and hybrid rocks associated with a PalaeoArchean layered ultramafic intrusion on the Johannesburg Dome, South Africa. *Journal of African Earth Sciences.* **102,** 203-217.

Arndt, N. T. 2013. Formation and Evolution of the Continental Crust. *Geochemical Perspectives.* **2** (3)

Attfield, P. 1987. Fluid inclusions in Scourian granulites from the Lewisian complex of NW Scotland: evidence for $CO_2$-rich fluid in Late Archean high-grade metamorphism. *Lithos,* **40,** 93-104.

Bagas L., Kolb, J., Fiorentini, M. L., Thebaud, N., Owen, J., Rennick, S., Stensgaard, B. M. 2016. On the processes that formed Archean Ni-Cu sulfide mineralisation in the deep continental crust, Thrym Complex, southeastern Greenland. *Precambrian Research.* **277,** 68-86.

Barnes, S. J., Roeder, P. L. 2001. The Range of Spinel Compositions in Terrestrial Mafic and Ultramafic Rocks. *Journal of Petrology.* **42** (12), 2279-2302.

Beach, A. 1973. The Mineralogy of High Temperature Shear Zones at Scourie, N.W. Scotland. *Journal of Petrology*, **14**, 231-248.

Bèdard, J. H., Harris, L. B., Thurston, P. C. 2013. The hunting of the snArc. *Precambrian Research.* **229,** 20-48.

Bédard, J. H. 2018. Stagnant lids and mantle overturns: Implications for Archean tectonics, magmagenesis, crustal growth, mantle evolution, and the start of plate tectonics. *Geoscience Frontiers.* **9,** 19-49.

BGS, 2011. [Shapefile geospatial data]. Scale 1:250,000, Tile: NC. Updated April 2011, Version 4, British Geological Survey, UK. Using: EDINA Geology Digimap Service, http://edina.ac.uk/digimap, Downloaded: February 2016.

Bowes, D. R., Wright, A. E. & Park, R. G. 1964. Layered intrusive rocks in the Lewisian of the North-West Highlands of Scotland. *Quarterly Journal of the Geological Society,* **120,** 153-192.

Brandl, G., Cloete, M., Anhaeusser, C. R. 2006. Archean Greenstone Belts. *The Geology of South Africa.* 9-56.

Brown, M. 2008. Characteristic thermal regimes of plate tectonics and their metamorphic imprint throughout Earth history: When did Earth first adopt a plate tectonics mode of behavior. *Special Paper of the Geological Society of America*. **440**, 97-128.

Burton, K. W., Capmas, F., Birck, J.-L., Allègre, C. J., Cohen, A. S. 2000. Resolving crystallisation ages of Archean mafic–ultramafic rocks using the Re–Os isotope system. *Earth and Planetary Science Letters,* **179,** 453-467.

Cartwright, I., fitches, W. R., O'Hara, M. J., barnicoat, A. C. & O'hara, S. 1985. Archean Supracrustal Rocks from the Lewisian near Stoer, Sutherland. *Scottish Journal of Geology*, **21**, 187–196.

Condie, K. C. 2005. High field strength element ratios in Archean basalts: a window to evolving sources of mantle plumes? *Lithos.* **79** (3-4), 491-504.

Corfu, F., Heaman, L. M., Rogers, G. 1994. Polymetamorphic evolution of the Lewisian complex, NW Scotland, as recorded by U-Pb isotopic compositions of zircon, titanite and rutile. *Contributions to Mineralogy and Petrology,* **117** (3), 215-228.

Crowley, Q. G., Key, R., Noble, S. R. 2014. High-precision U–Pb dating of complex zircon from the Lewisian Gneiss Complex of Scotland using an incremental CA-ID-TIMS approach. *Gondwana Research,* **27** (4), 1381-1391.

Davies, F. B. 1974. A layered basic complex in the Lewisian, south of Loch Laxford, Sutherland. *Journal of the Geological Society,* **130,** 279-284.

Davies, J. H. F. L. & Heaman, L. M. 2014. New U–Pb baddeleyite and zircon ages for the Scourie dyke swarm: A long-lived large igneous province with implications for the Paleoproterozoic evolution of NW Scotland. *Precambrian Research,* **249,** 180-198.

De Wit, M. J., Hart, R. A., Hart, R. J. 1987. The Jamestown Ophiolite Complex, Barberton mountain belt: a section through 3.5 Ga oceanic crust. *Journal of African Earth Sciences.* **6** (5), 681-730.

De Wit, M. J., Roering, C., Hart, R. J., Armstrong, R. A., De Ronde, C. E. J., Green, R. W. E., Tredoux, M., Peberdy, E., Hart, R. A. 1992. Formation of an Archean continent. *Nature.* **357,** 553-562

Droop, G. T. R. 1987. A general equation for estimating $Fe^{3+}$ concentrations in ferromagnesian silicates and oxides from microprobe analyses, using stoichiometric criteria. *Mineralogical Magazine,* **51,** 431-435.

Evans, C. R. 1965. Geochronology of the Lewisian basement near Lochinver, Sutherland. *Nature*, 207, 54–55.

Evans, C. R., Lambert, R. S. J. 1974 The Lewisian of Lochinver, Sutherland; the type area for the Inverian metamorphism. *Journal of the Geological Society.* **130,** 125-150

Friend, C. & Kinny, P. 2001. A reappraisal of the Lewisian Gneiss Complex: geochronological evidence for its tectonic assembly from disparate terranes in the Proterozoic. *Contributions to Mineralogy and Petrology,* **142,** 198-218.

Furness, H., Rosing, M., Dilek, Y., De Wit, M. 2009. Isua supracrustal belt (Greenland)—A vestige of a 3.8 Ga suprasubduction zone ophiolite, and the implications for Archean geology. *Lithos.* **113,** 115-132.

Furness, H., Dilek, Y., De Wit, M. 2015. Precambrian greenstone sequences represent different ophiolite types. *Gondwana Research.* **27,** 649-685

Goodenough K. M. & Krabbendam, M. 2011. A Geological Excursion Guide to the North-West Highlands of Scotland. Edinburgh Geological Society, Edinburgh.

Goodenough, K. M., Park, R. G., Krabbendam, M., Myers, J. S.*,* Wheeler, J., Loughlin, S. C., Crowley, Q. G., Friend, C. R. L., Beach, A., Kinny, P. D., Graham, R. H. 2010. The Laxford Shear Zone: an end-Archean terrane boundary? *Geological Society, London, Special Publications,* **335,** 103-120.

Goodenough, K. M., Crowley, Q. G., Krabbendm, M., Parry, S. F. 2013. New U-Pb age constraints for the Laxford Shear Zone, NW Scotland: Evidence for tectono-magmatic processes associated with the formation of a Paleoproterozoic supercontinent. *Precambrian Research,* **223,** 1-19.

Harris, L. B., Bèdard, J. H. 2014. Crustal Evolution of Deformation in a Non-Plate-Tectonic Archean Earth: Comparisons with Venus. *In:* Dilek, Y., Furnes, H. (eds) Evolution of Archean Crust and Early Life. Modern Approaches in Solid Earth Sciences. **7.** Springer, Dordrecht.

Heaman, L. M., Tarney, J. 1989. U–Pb Baddeleyite ages for the Scourie Dyke Swarm, Scotland – evidence for 2 distinct intrusion events. Nature, **340,** 705–708.

Hoatson, D. M., Sun, S-S. 2002. Archean Layered Mafic-Ultramafic Intrusions in the West Pilbara
Craton, Western Australia: A Synthesis of Some of the Oldest Orthomagmatic Mineralizing
Systems in the World. *Economic Geology.* **97,** 847-872.

Hughes, H. S. R., McDonald, I., Goodenough, K. M., Ciborowski, T. J. R., Kerr, A. C., Davies, J. H. F. L.,
Selby, D. 2014. Enriched lithospheric mantle keel below the Scottish margin of the North
Atlantic Craton: Evidence from the Palaeoproterozoic Scourie Dyke Swarm and mantle
xenoliths. *Precambrian Research,* **250,** 97-126.

Ivanic, T. J., Wingate, M. T. D., Kirkland, C. L., Van Kranendonk, M. J., Wyche, S. 2010. Age and
significance of voluminous mafic-ultramafic magmatic events in the Murchison Domain,
Yilgarn Craton. *Australian Journal of Earth Sciences.* **57,** 597-614.

Ivanic, T. J., Nebel, O., Brett, J., Murdie, R. E. 2017. The Windimurra Igneous Complex: an Archean
Bushveld? From: Gessner, K., Blenkinsop, T. G. & Sorjonen-Ward, P. Characterization of Ore-
Forming Systems from Geological, Geochemical and Geophysical Studies. *Geological Society,
London, Special Publications*, 453.

Johnson, T. E., White, R. W. 2011. Phase equilibrium constraints on conditions of granulite-facies
metamorphism at Scourie, NW Scotland. *Journal of the Geological Society, London,* **168,** 147-
158.

Johnson, T. E., Fischer, S., White, R. W., Brown, M*., et al.* 2012. Archean Intracrustal Differentiation
from Partial Melting of Metagabbro--Field and Geochemical Evidence from the Central
Region of the Lewisian Complex, NW Scotland. *Journal of Petrology,* **53,** 2115-2138.

Johnson, T. E., Fischer, S. & White, R. W. 2013. Field and petrographic evidence for partial melting of
TTG gneisses from the central region of the mainland Lewisian complex, NW Scotland.
*Journal of the Geological Society,* **170,** 319-326.

Johnson, T. E., Brown, M., Goodenough, K. M., Clark, C., Kinny, P. D., White, R. W. 2016. Subduction or sagduction? Ambiguity in constraining the origin of ultramafic-mafic bodies in the Archean crust of NW Scotland. *Precambrian Research,* **283,** 85-105.

Johnson, T. E., Brown, M., Gardiner, N. J., Kirkland, C. L., Smithies, H. 2017. Earth's first stable continents did not form by subduction. *Nature.* **543,** 239-242.

Josey, I. K., Shaw, N. D. 1974. Discussion of a layered basic complex in the Lewisian. *Journal of the Geological Society,* **130,** 595-597.

Kamber, B. S. 2015. The evolving nature of terrestrial crust from the Hadean, through the Archean, into the Proterozoic. *Precambrian Research.* **258,** 48-82.

Kinny, P. D. & Friend, C. R. L. 1997. U-Pb isotopic evidence for the accretion of different crustal blocks to form the Lewisian Complex of northwest Scotland. *Contributions to Mineralogy and Petrology,* **129,** 326-340.

Kinny, P. D., Friend, C. R. L. & Love, G. J. 2005. Proposal for a terrane-based nomenclature for the Lewisian Gneiss Complex of NW Scotland. *Journal of the Geological Society,* **162,** 172-186.

Kolb, J., Thrane, K., Bagas, L. 2013. Field relationship of high-grade Neo- to MesoArchean rocks of South-East Greenland: Tectonometamorphic and magmatic evolution. *Gondwana Research.* **23,** 471-492.

Kolb, J., Bagas, L., Fiorentini, M. L. 2015. Metallogeny of the North Atlantic Craton in Greenland. *Mineralogical Magazine.* **79,** 815-855.

Love, G. J., Kinny, P. D. & Friend, C. R. L. 2004. Timing of magmatism and metamorphism in the Gruinard Bay area of the Lewisian Gneiss Complex: comparisons with the Assynt Terrane and implications for terrane accretion. *Contributions to Mineralogy and Petrology,* **146,** 620-636.

Love, G. J., Friend, C. R. L. & Kinny, P. D. 2010. Palaeoproterozoic terrane assembly in the Lewisian Gneiss Complex on the Scottish mainland, south of Gruinard Bay: SHRIMP U–Pb zircon evidence. *Precambrian Research,* **183,** 89-111.

MacDonald, J. M., Wheeler, J., Harley, S. L., Mariani, E., Goodenough, K. M., Crowley, Q., Tatham, D. 2013. Lattice distortion in a zircon population and its effects on trace element mobility and U–Th–Pb isotope systematics: examples from the Lewisian Gneiss Complex, northwest Scotland. *Contributions to Mineralogy and Petrology,* **166,** 21-41.

MacDonald, J. M., Goodenough, K. M., Wheeler, J., Crowley, Q*., et al.* 2015. Temperature–time evolution of the Assynt Terrane of the Lewisian Gneiss Complex of Northwest Scotland from zircon U-Pb dating and Ti thermometry. *Precambrian Research,* **260,** 55-75.

Myers, J.S., 1985. Stratigraphy and structure of the Fiskenæsset Complex, southern West Greenland. Geol. Survey Greenland Rep. 150, 72 pp.

Namur, O., Abily, B., Boudreau, A.E., Blanchette, F., Bush, J.W.M., Ceulenneer, G., Charlier, B., Donaldson, C.H., Duchesne, J.-C., Higgins, M.D., Morata, D., Neilsen, T.F.D., O'Driscoll, B., Pang, K.N., Peacock, T., Spandler, C.J., Toramaru, A., Veksler, I. V., 2015. Igneous Layering in Basaltic Magma Chambers, in: Charlier, B. Namur., O., Latypov, R., Tegner, C. Layered Intrusions. Springer Geology, Pp. 75-152.

Nutman, A. P., Bennett, V. C., Friend, C. R. L., Hidaka, H., Yi, K., Lee, S. R., Kamiichi, T. 2013. The Itsaq Gneiss Complex Of Greenland: Episodic 3900 To 3660 Ma Juvenile Crust Formation And Recycling In The 3660 To 3600 Ma Isukasian Orogeny. *American Journal of Science.* **313,** 877-911

O'Hara, M. J. 1961. Zoned Ultrabasic and Basic Gneiss Masses in the Early Lewisian Metamorphic Complex at Scourie, Sutherland. *Journal of Petrology,* **2,** 248-276.

Park, R. G. 1964. The structural history of the Lewisian Rocks of Gairloch, Wester Ross. Quarterly
*Journal of the Geological Society, London*, **120**, 397–434.

Park, R. G. 1970. Observations on Lewisian chronology. *Scottish Journal of Geology, 6,* 379-399.

Park, R. G. 1991. The Lewisian Complex. In: Craig, G. Y. (ed.) *Geology of Scotland*. Alden Press,
Oxford, UK.

Park, R. G. 2005. The Lewisian terrane model : a review. *Scottish Journal of Geology, 41,* 105-118.

Park, R. G. & Tarney, J. 1987. The Lewisian complex: a typical Precambrian high-grade terrain?
*Geological Society Special Publication, 27,* 13-25.

Park R. G., Stewart, A. D., Wright, D. T. 2002. The Hebridean terrane. In: Trewin, N. H. (ed.) The
*Geology of Scotland.* Geological Society, London, 45–80.

Peach, B. N., Horne, J., Gunn, W., Clough, C. T., Hinxman, L. W., Teall, J. J. H. 1907.  The Geological
Structure of the North-West Highlands of Scotland. *Memoir of the Geological Survey of Great
Britain*. HMSO, Glasgow.

Polat, A., Appell, P. W. U., Fryer, B., Windley, B., Frei, R., Samson, I. M., Hung, H. 2009. Trace element
systematics of the Neoarchean Fiskenæsset anorthosite complex and associated meta-
volcanic rocks, SW Greenland: Evidence for a magmatic arc origin. *Precambrian Research.
175,* 87-115.

Rollinson, H. R. & Windley, B. F. 1980. An Archean granulite-grade tonalite-trondhjemite-granite
suite from scourie, NW Scotland: Geochemistry and origin. *Contributions to Mineralogy and
Petrology, 72,* 265-281.

Rollinson, H. R. & Fowler, M. B. The magmatic evolution of the Scourian complex at Gruinard Bay. In:
Park, R. G. & Tarney, J. (eds), 1987, Evolution of the Lewisian and Comparable Precambrian
High Grade Terrains, *Geological Society Special Publication*, **27**, 57-71.

Rollinson, H. & Gravestock, P. 2012. The trace element geochemistry of clinopyroxenes from pyroxenites in the Lewisian of NW Scotland: insights into light rare earth element mobility during granulite facies metamorphism. *Contributions to Mineralogy and Petrology,* **163,** 319-335.

Sheraton, J. W., Skinner, A. C., Tarney, J. 1973. The geochemistry of the Scourian gneisses of the Assynt district. *The early Precambrian of Scotland and related rocks of Greenland.* 13-30.

Sills, J. D. 1981. Geochemical studies of the Lewisian Complex of the Western Assynt Region, N. W. Scotland. *PhD thesis*. University of Leicester.

Sills, J. D., Savage, D., Watson, J. V. & Windley, B. F. 1982. Layered ultramafic-gabbro bodies in the Lewisian of northwest Scotland: geochemistry and petrogenesis. *Earth and Planetary Science Letters,* **58,** 345-360.

Stern, R. J. 2005. Evidence from ophiolites, blueschists, and ultrahigh-pressure metamorphic terranes that the modern episode of subduction tectonics began in Neoproterozoic. *Geology.* **33** (7), 557-560.

Stern, R. J. 2008. Modern-style plate tectonics began in Neoproterozoic time: An alternative interpretation of Earth's tectonic history. *Special Paper of the Geological Society of America*. **440,** 265-280.

Sutton, J. & Watson, J. V. 1951. The pre-Torridonian metamorphic history of the Loch Torridon and Scourie areas in the northwest Highlands, and its bearing on the chronological classification of the Lewisian. *Quarterly Journal of the Geological Society,* **106,** 241-307.

Szilas, K., Van Hinsberg, V. J., Kisters, A. F. M., Hoffmann, J. E., Windley, B. F., Kokfelt, T. F., Scherstèn, A., Frei, R., Rosing, M. T., Münker, C. 2013. Remnants of arc-related MesoArchean oceanic crust in the Tartoq Group of SW Greenland. *Gondwana Research.* **23,** 436-451.

Szilas, K., Van Hinsberg, V. J., Creaser, R. A., Kisters, A. F. M. 2014. The geochemical composition of serpentinites in the MesoArchean Tartoq Group, SW Greenland: Harzburgitic cumulates or melt-modified mantle? *Lithos.* **198-199,** 103-116.

Szilas, K., Van Hinsberg, V., McDonald, I., Nærra, T., Rollinson, H., Adetunji, J., Bird, D. Highly refractory Archean peridotite cumulates: Petrology and geochemistry of the Seqi Ultramafic Complex, SW Greenland. *In press. Geoscience Frontiers.*

Timms, N. E., Kinny, P. D., Reddy, S. M. 2006. Enhanced diffusion of Uranium and Thorium linked to crystal plasticity in zircon. *Geochemical Transactions.* **7** (10)

Van Kranendonk. M. J., Collins, W. J.., Hickman, A., Pawley, M. J. 2004. Critical tests of vertical vs. Horizontal tectonic models for the Archean East Pilbara Granite-Greenstone Terrane, Pilbara Craton, Western Australia. *Precambrian Research.* **131,** 173-211.

Wang, D., Guo, J., Huang, G., Scheltens, M. 2015. The Neoarchean ultramafic–mafic complex in the Yinshan Block,North China Craton: Magmatic monitor of development of Archean lithospheric mantle. *Precambrian Research,* **270,** 80-99.

Warren, J. M. 2016. Global variations in abyssal peridotite compositions. *Lithos,* **248-251,** 193-219.

Weaver, B.L., Tarney, J., 1981. The Scourie Dyke Suite: petrogenesis and geochemical nature of the Proterozoic sub-continental mantle. *Contributions to Mineralogy and Petrology,* **78,** 175–188.

Wheeler, J., Park, R. G., Rollinson, H. R. & Beach, A. 2010. The Lewisian Complex: insights into deep crustal evolution. *Geological Society, London, Special Publications,* **335,** 51-79.

Whitehouse, M. J. 1989. Sm-Nd evidence for diachronous crustal accretion in the Lewisian complex of northwest Scotland. *Tectonophysics,* **161,** 245-256.

Whitehouse, M. J., Fedo, C. M. 2003. Deformation features and critical field relationships of early Archean rocks, Akilia, southwest Greenland. *Precambrian Research.* **126,** 2259-271.

38

Whitehouse, M. J. & Kemp, A. I. S. 2010. On the difficulty of assigning crustal residence, magmatic protolith and metamorphic ages to Lewisian granulites: constraints from combined in situ U-Pb and Lu-Hf isotopes. *Geological Society, London, Special Publications,* **335,** 81-101.

Zirkler, A., Johnson, T. E., White, R. W., Zack, T. 2012. Polymetamorphism in the mainland Lewisian complex, NW Scotland – phase equilibria and geochronological constraints from the Cnoc an t'Sidhean suite. *Journal of Metamorphic Geology,* **30,** 865-885.

**FIGURE CAPTIONS**

Fig. 1: Basic geological map of the LGC, detailing the location of the Ben Strome and Geodh' nan Sgadan Complexes within the Central Region, alongside the location of other ultramafic-mafic complexes (redrawn after: Kinny and Friend, 1997; Kinny et al., 2005; Goodenough et al., 2010, 2013; Johnson et al., 2016). Abbreviations: CG=Cnoc Gorm; GC=Ghnoc Gorm; NSB=North Scourie Bay; Sm=Scouriemore (includes Camas nam Buth); LD=Lochan Daihm Mor; LEC=Loch Eilean na Craoibhe Moire; BD=Ben Dreavie; Db=Drumbeg; Av=Achmelvich; Ab=Achiltibuie; GB=Gruinard Bay; Ct=Clachtoll; St=Strathan; LSZ=Laxford Shear Zone; GSZ=Gairloch Shear Zone.

Fig. 2: (a) Simplified geological map of the Ben Strome Complex, including representative structural measurements; (b) detailed geological map of a re-folded fold in the Leathaid Domain; (c) form surface map of the Leathaid Domain and Laxfordian shear zone. Black lines represent TTG gneissosity. Blue lines represent igneous layering; (d) Cross-section from A-A$^|$ detailing the structure of the Ben Strome Complex in the Maldie Domain and interaction with the Laxfordian shear zone (LSZ); (e) Cross-section from B-B$^|$, detailing the structure of the Ben Strome Complex in the Leathaid Domain.

Fig. 3: Field photographs detailing representative rock types and field relationships in the Ben Strome Complex and surrounding TTG gneiss. (a) Gradational contact between layered metapyroxenite and garnet-metagabbro in the Maldie River, Maldie Domain. (b) Layered websterite and olivine-websterite overlain by heterogeneous garnet-metagabbro and metagabbro, Maldie Domain. (c) Relationship between TTG gneiss and overlying Ben Strome Complex, Maldie Domain. Note: S1 gneissosity is parallel to layering of metawebsterite and meta-olivine-websterite. (d) steeply-dipping, centimetre-scale Laxfordian foliation. (e) layered meta-olivine-websterite (brown and internally layered on the millimetre-scale) and metawebsterite (grey and blocky), Maldie Domain. (f) millimetre to metre-scale modal layering of metapyroxenite and metaperidotite, Leathaid Domain, with a combination of gradational and sharp contacts. (g) garnet-metagabbro, Leathaid Domain. (h) metagabbro, with relict igneous layering preserved. Leathaid Domain. (i) plagioclase and pyroxene-rich leucosome cross-cutting garnet-metagabbro, Maldie Domain. (j) TTG-derived quartz-rich leucosome cross-cutting Ben Strome Complex metagabbro, Leathaid Domain. Hammer length = 40 cm; hammer head width = 17 cm.

Fig. 4: Stereonet (lower hemisphere projection) of structures in and around the Ben Strome Complex.

Fig. 5: Field photographs detailing the outcrop-scale folding of the S1 gneissosity in the Leathaid Domain.

Fig. 6: Ternary plot detailing the modal mineral percentages of ultramafic rocks in the Ben Strome Complex.

Fig. 7: Photomicrographs detailing representative rocks types of the Ben Strome Complex rocks. With the exception of photomicrographs (b) and (e), which are taken using plane-polarised light, all photomicrographs are taken using crossed-polarised light. (a) serpentinsed metalherzolite, including remnants of olivine; (b) serpentinised metalherzolite, including remnants of olivine; (c) meta-olivine-websterite, including 120° triple junction grain boundaries; (d) metawebsterite, including 120° triple

40

junction grain boundaries; (e) meta-olivine-websterite; (f) meta-olivine-websterite; (g) garnet-metagabbro, (h) amphibolite, including 120° triple junction grain boundaries and finer-grained areas of plagioclase and amphibole. Abbreviations: srp=serpentine; am=amphibole; ol=olivine; cpx=clinopyroxene; opx=orthopyroxene; plag=plagioclase; spn=spinel; gt=garnet. White scale bar=1 mm.

Fig. 8: Photomicrographs detailing representative spinel analysed in the metapyroxenites. Abbreviations: spn=spinel; cpx=clinopyroxene; opx=orthopyroxene; am=amphibole. Black scale bar=500 μm.

Fig. 9: Spinel compositions for the Ben Strome Complex. Representative analyses can be found in Table 2 and the full dataset is available in the supplementary material.

Fig. 10: (a) Simplified geological map of the Geodh' nan Sgadan locality (this study). Inset: location map, detailing the location relative to Badcall Bay and the A894 road; (b) stratigraphic log from A to B (this study). Line of transect can be found on (a); (c) geological map of the Geodh' nan Sgadan locality, redrawn after: Rollinson and Windley (1980).

Fig. 11: Field photographs detailing the representative rock types and field relationships at the Geodh' nan Sgadan locality. (a) TTG gneiss containing mafic pods; (b) juxtaposition of mafic rocks and TTG gneiss by fault; (c) well-defined layering marked by centimetre-scale layers of metapyroxenite in metagabbro; (d) centimetre-scale garnet-metagabbro layer; (e) poorly-developed layering in metagabbro, with some truncation of layers; (f) plagioclase-rich leucosome cross-cutting poorly-developed layering in metagabbro. (g) plagioclase-rich leucosome cross-cutting subtly layered metagabbro. (h) 1.5 m thick sheet of trondhjemite. Yellow hammer length = 40 cm; yellow hammer head width = 17 cm.

Fig. 12: Representative photomicrographs detailing the petrographic characteristics of the Geodh' nan Sgadan mafic rocks. All photomicrographs are taken using crossed-polarised light. (a) metagabbro, including thick rims of amphibole surrounding clinopyroxene. (b) metagabbro

containing near-complete alteration of clinopyroxene to amphibole. (c) metagabbro containing relatively large, unaltered clinopyroxene and plagioclase. (d) metagabbro, including partial alteration of plagioclase. Abbreviations: cpx = clinopyroxene; opx = orthopyroxene; pl = plagioclase. White scale bar = 1 mm.

Fig. 13: Schematic diagram detailing the geotectonic environments potentially responsible for forming the various ultramafic-mafic components of the LGC.

**TABLES AND TABLE CAPTIONS**

Table 1: Summary of the basic characteristics of selected Archean ultramafic-mafic complexes from the North Atlantic, Kaapvaal, Yilgarn and North China Cratons. References listed by complex.

| Ultramafic-mafic complex | Age (Ga) | Size (km²) | Lithological assemblage | Age relationship with host rocks | Metamorphic grade | Interpretation(s) | Key references |
|---|---|---|---|---|---|---|---|
| *North Atlantic Craton – Greenland* | | | | | | | |
| Thrym | 2.85-2.75 | >70 | Mafic & intrusive ultramafic | Invaded by orthogneiss | Granulite | Ultramafic intrusions into a pre-existing mafic crust. | Kolb et al., 2013; Bagas et al., 2016 |
| Fiskenæsset | 2.97 | ~ 100 | Intrusive and extrusive mafic and ultramafic | Invaded by orthogneiss | Amphibolite to granulite | Arc-related sills emplaced into oceanic crust comprising basalt & gabbro | Myers, 1985; Polat et al., 2009 |
| Seqi | >2.97 | <0.5 | Intrusive ultramafic | Invaded by orthogneiss | Granulite | Mantle residues following high degrees of partial melting | Szilas et al., 2017 |
| Tartoq | ~3.1 | 50 | Intrusive ultramafic | Invaded by orthogneiss | Greenschist to granulite | Remnants of oceanic crust that formed in a suprasubduction zone setting. | Szilas et al., 2013, 2014 |
| Akilia | ? | <0.5 | Ultramafic-mafic- rocks | Unknown – surrounded by orthogneiss | Granulite | ? | Whitehouse and Fedo, 2003 |
| *Kaapvaal Craton* | | | | | | | |

| Stolzburg | >3.25 | ~ 15 | Intrusive ultramafic-mafic rocks | Debated – intrusive into schist belt or tectonically juxtaposed? | Amphibolite | Layered intrusion; accreted oceanic crust | De Wit et al., 1987; Anhaeusser, 2001 |
|---|---|---|---|---|---|---|---|
| Koedoe | 3.5-3.2 | ~15 | Intrusive ultramafic | Intruded Barberton greenstone belt | Greenschist | Layered intrusion; accreted oceanic crust | Anhaeusser, 2006b |
| Zandspruit | >3.11 | 0.5 | Intrusive ultramafic-mafic and greenstone | Invaded by TTG | Amphibolite | Layered intrusion emplaced into greenstone remnant; accreted oceanic crust | Anhaeusser, 2006a; Anhaeusser, 2015 |
| **Yilgarn Craton** | | | | | | | |
| Windimurra | 2.7-2.8 | 2500 | Intrusive | Intrusion into greenstone belt | Greenschist | Plume-related layered Intrusion | Ivanic et al., 2010; Ivanic et al., 2017 |
| Munni Munni | 2.93 | >100 | Intrusive ultramafic-mafic | Intruded granite-supracrustal sequence contact | Greenschist | Layered intrusion; magma generated by melting oceanic crust | Hoatson and Sun, 2002 |
| **North China Craton** | | | | | | | |
| Yinshan | 2.6 | 10 | Intrusive ultramafic - mafic rocks | Invaded by TTG | Amphibolite to granulite | Subduction-related, multi-phase, intrusion | Wang et al., 2015 |

Table 2: Representative quantitative analyses of spinel from the Ben Strome Complex. Analyses are from 7 metapyroxenite thin sections and the full dataset, including sample locations, is available in the supplementary material.

Table 2

| Thin section | LW16-Z6 | LW16-Z6 | LW16-Y11 | LW16-Y11 | LW16-Y8B | LW16-Y8B | LW16-Z11I | LW16-Z11I |
|---|---|---|---|---|---|---|---|---|
| Domain | Leathaid | Leathaid | Maldie | Maldie | Maldie | Maldie | Leathaid | Leathaid |
| $SiO_2$ (%) | 0.30 | 0.30 | 0.30 | 0.26 | 0.30 | 0.30 | 0.28 | 0.32 |
| $TiO_2$ (%) | 0.62 | 0.65 | 0.18 | 0.10 | 0.22 | 0.27 | 0.07 | 0.05 |
| $Al_2O_3$ (%) | 1.02 | 1.27 | 0.49 | 0.47 | 0.49 | 0.55 | 0.51 | 0.36 |
| FeO (%) | 36.84 | 36.98 | 35.30 | 34.98 | 34.30 | 34.69 | 34.28 | 33.70 |
| $Fe_2O_3$ (%) | 53.52 | 52.41 | 57.43 | 58.02 | 60.04 | 59.17 | 59.78 | 60.14 |
| MnO (%) | 0.22 | 0.23 | 0.18 | 0.18 | 0.15 | 0.15 | 0.18 | 0.17 |
| MgO (%) | 0.71 | 0.70 | 0.60 | 0.61 | 0.66 | 0.63 | 0.65 | 0.68 |
| $Cr_2O_3$ (%) | 5.01 | 5.36 | 3.98 | 3.83 | 2.25 | 2.59 | 2.65 | 2.27 |
| $V_2O_3$ (%) | 0.49 | 0.46 | 0.29 | 0.34 | 0.60 | 0.63 | 0.59 | 0.49 |
| NiO (%) | 0.69 | 0.74 | 0.52 | 0.46 | 0.84 | 0.83 | 0.31 | 0.45 |
| TOTAL | 99.42 | 99.09 | 99.28 | 99.25 | 99.86 | 99.81 | 99.28 | 98.62 |
| | | | | | | | | |
| **Cations on the basis of 4 oxygens** | | | | | | | | |
| Si | 0.01 | 0.01 | 0.01 | 0.01 | 0.01 | 0.01 | 0.01 | 0.02 |
| Ti | 0.02 | 0.02 | 0.01 | 0.00 | 0.01 | 0.01 | 0.00 | 0.00 |
| Al | 0.05 | 0.06 | 0.02 | 0.02 | 0.02 | 0.02 | 0.02 | 0.02 |
| $Fe^{2+}$ | 1.17 | 1.17 | 1.13 | 1.12 | 1.09 | 1.10 | 1.10 | 1.09 |
| $Fe^{3+}$ | 1.53 | 1.50 | 1.65 | 1.67 | 1.72 | 1.69 | 1.72 | 1.74 |
| Mn | 0.01 | 0.01 | 0.01 | 0.01 | 0.01 | 0.01 | 0.01 | 0.01 |

43

| | | | | | | | |
|---|---|---|---|---|---|---|---|
| Mg | 0.05 | 0.05 | 0.04 | 0.05 | 0.05 | 0.05 | 0.05 | 0.05 |
| Cr | 0.19 | 0.20 | 0.16 | 0.15 | 0.09 | 0.10 | 0.10 | 0.09 |
| V | 0.02 | 0.02 | 0.01 | 0.01 | 0.02 | 0.03 | 0.02 | 0.02 |
| Ni | 0.03 | 0.03 | 0.02 | 0.02 | 0.03 | 0.03 | 0.01 | 0.02 |
| TOTAL | 3.07 | 3.07 | 3.06 | 3.06 | 3.05 | 3.05 | 3.05 | 3.05 |
| | | | | | | | | |
| Mg# | 1.87 | 1.84 | 1.56 | 1.60 | 1.71 | 1.63 | 1.68 | 1.77 |
| Cr# | 80.79 | 78.33 | 87.53 | 87.57 | 80.01 | 80.44 | 81.91 | 84.68 |
| $Fe^{2+}$# | 0.96 | 0.96 | 0.96 | 0.96 | 0.96 | 0.96 | 0.96 | 0.96 |
| $Fe^{3+}$# | 0.87 | 0.85 | 0.90 | 0.91 | 0.94 | 0.93 | 0.93 | 0.94 |

Table 2 (cont.)

| Thin Section | Lw16-Z11c(1) | Lw16-Z11c(1) | Lw16-Z11c(2) | Lw16-Z11c(2) | Lw16-Z11c(2) | Lw16-Z11g(1) | Lw16-Z11g(1) |
|---|---|---|---|---|---|---|---|
| Domain | Leathaid | Leathaid | Leathaid | Leathaid | Leathaid | Leathaid | Leathaid |
| $SiO_2$ (%) | 0.24 | 0.30 | 0.28 | 0.28 | 0.30 | 0.30 | 0.28 |
| $TiO_2$ (%) | 0.08 | 0.12 | 0.08 | 0.12 | 0.08 | 0.10 | 0.08 |
| $Al_2O_3$ (%) | 0.40 | 0.43 | 0.43 | 0.40 | 0.38 | 0.42 | 0.42 |
| FeO (%) | 32.23 | 34.52 | 34.11 | 33.76 | 33.77 | 34.66 | 34.76 |
| $Fe_2O_3$ (%) | 59.86 | 57.72 | 59.70 | 59.79 | 59.89 | 57.34 | 57.47 |
| MnO (%) | 0.09 | 0.13 | 0.13 | 0.10 | 0.12 | 0.17 | 0.14 |
| MgO (%) | 0.45 | 0.60 | 0.53 | 0.55 | 0.48 | 0.71 | 0.70 |
| $Cr_2O_3$ (%) | 3.51 | 3.36 | 2.59 | 2.29 | 2.34 | 3.52 | 3.57 |
| $V_2O_3$ (%) | 0.59 | 0.49 | 0.55 | 0.55 | 0.50 | 0.57 | 0.63 |
| NiO (%) | 0.76 | 0.75 | 0.60 | 0.62 | 0.65 | 0.61 | 0.64 |
| TOTAL | 98.20 | 98.41 | 99.00 | 98.46 | 98.51 | 98.40 | 98.68 |
| **Cations on the basis of 4 oxygens** | | | | | | | |
| Si | 0.01 | 0.01 | 0.01 | 0.01 | 0.02 | 0.01 | 0.01 |
| Ti | 0.00 | 0.00 | 0.00 | 0.00 | 0.00 | 0.00 | 0.00 |
| Al | 0.02 | 0.02 | 0.02 | 0.02 | 0.02 | 0.02 | 0.02 |
| $Fe^{2+}$ | 1.05 | 1.11 | 1.09 | 1.09 | 1.09 | 1.12 | 1.12 |
| $Fe^{3+}$ | 1.75 | 1.67 | 1.72 | 1.74 | 1.74 | 1.66 | 1.66 |
| Mn | 0.00 | 0.01 | 0.01 | 0.00 | 0.00 | 0.01 | 0.01 |
| Mg | 0.03 | 0.04 | 0.04 | 0.04 | 0.04 | 0.05 | 0.05 |
| Cr | 0.14 | 0.13 | 0.10 | 0.09 | 0.09 | 0.14 | 0.14 |
| V | 0.02 | 0.02 | 0.02 | 0.02 | 0.02 | 0.02 | 0.03 |
| Ni | 0.03 | 0.03 | 0.02 | 0.03 | 0.03 | 0.02 | 0.03 |
| TOTAL | 3.06 | 3.06 | 3.05 | 3.05 | 3.05 | 3.06 | 3.06 |

44

| Mg# | 1.19 | 1.57 | 1.38 | 1.43 | 1.26 | 1.87 | 1.83 |
| Cr# | 88.50 | 87.07 | 83.88 | 83.50 | 84.41 | 88.05 | 88.18 |
| $Fe^{2+}$# | 0.97 | 0.96 | 0.97 | 0.96 | 0.97 | 0.95 | 0.96 |
| $Fe^{3+}$# | 0.92 | 0.92 | 0.93 | 0.94 | 0.94 | 0.91 | 0.91 |

(a) garnet-metagabbro

irregular, gradational contact

pyroxenite

(b) garnet-metagabbro and metagabbro

layered websterite and olivine-websterite

mm-scale layering dips 22° N

W          E

(c) garnet-metagabbro and gabbro

layered websterite and olivine-websterite

S1 gneissosity

TTG gneiss

(d) Laxfordian foliation

(e) websterite

olivine websterite, with mm-scale layering

(f) peridotite          pyroxenite
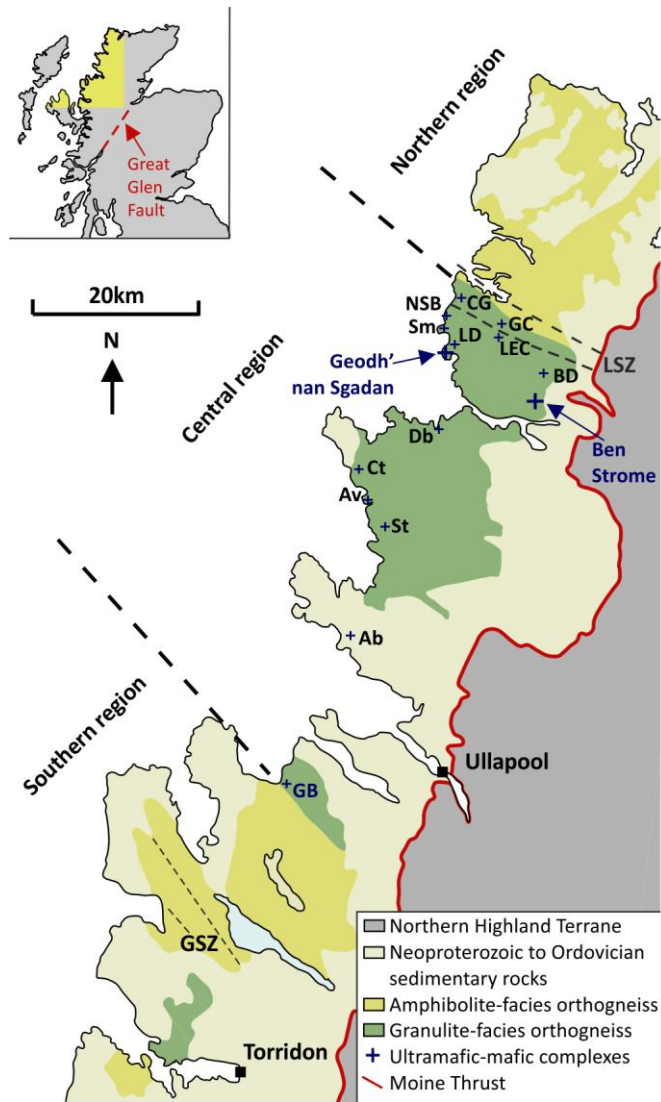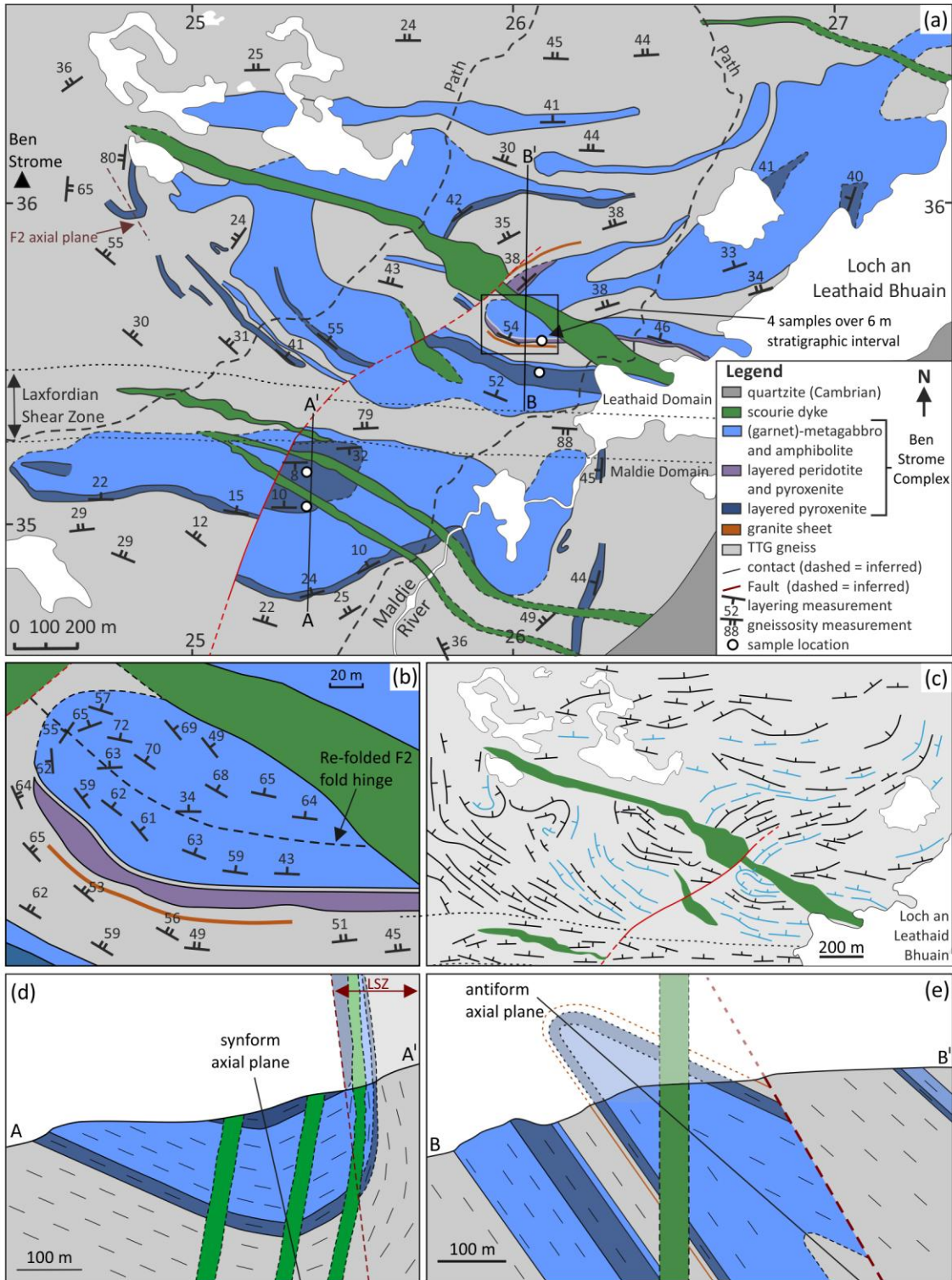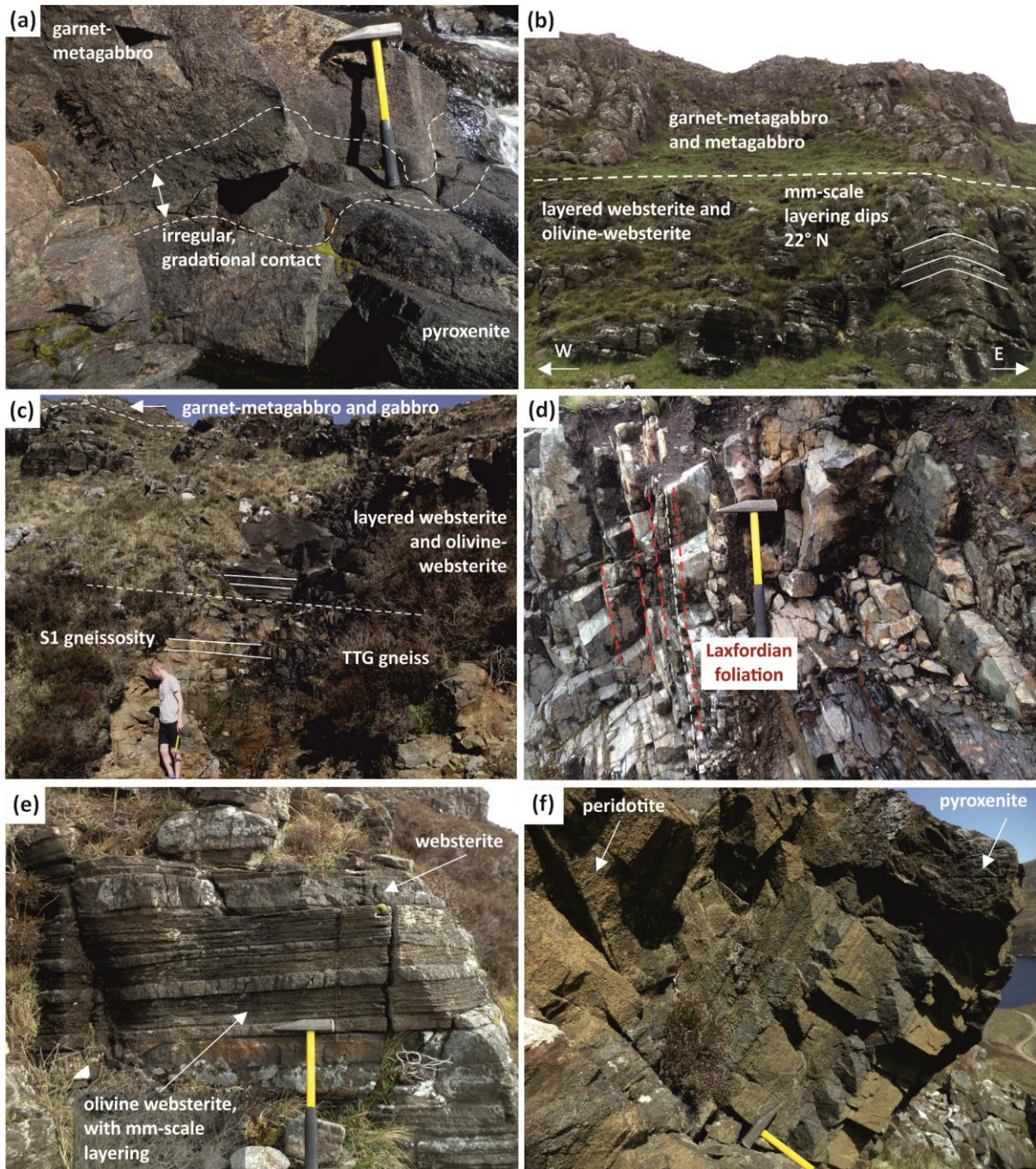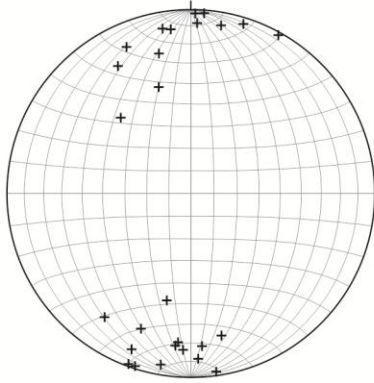
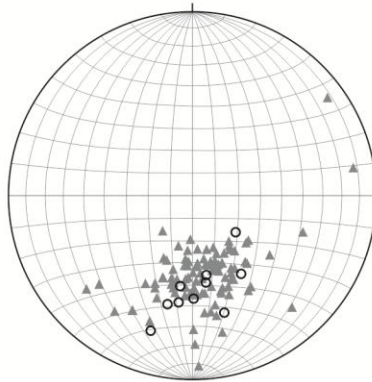(a) Laxfordian shear zone  (b) Maldie Domain - west  (c) Maldie Domain - east
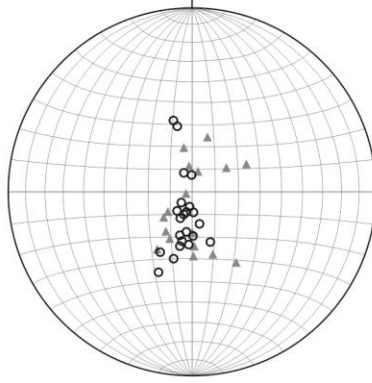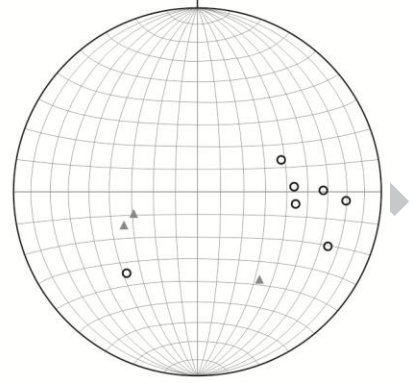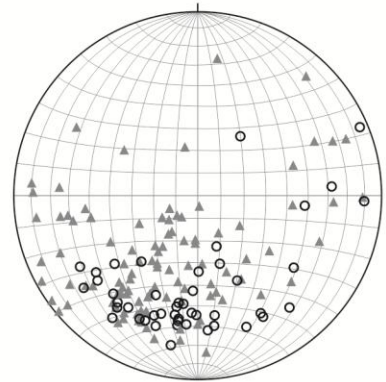
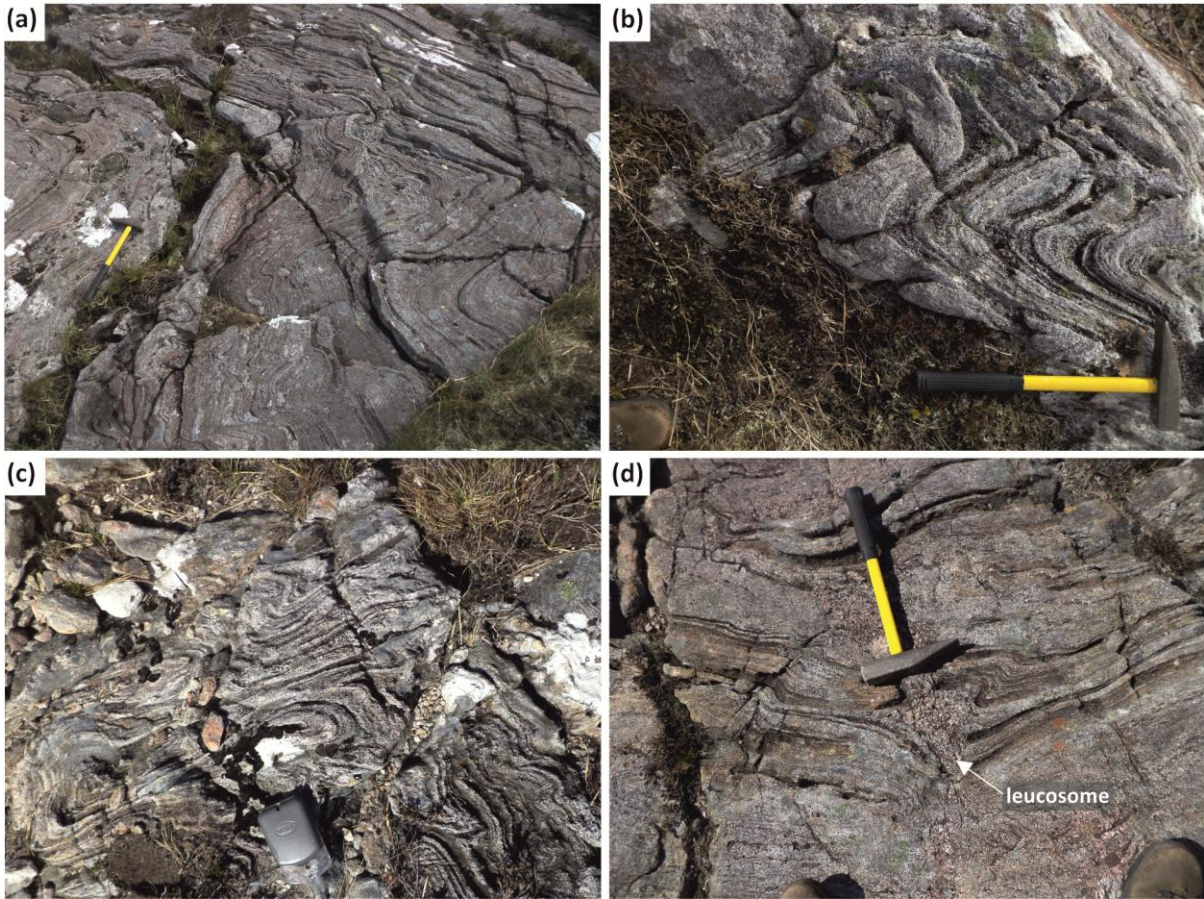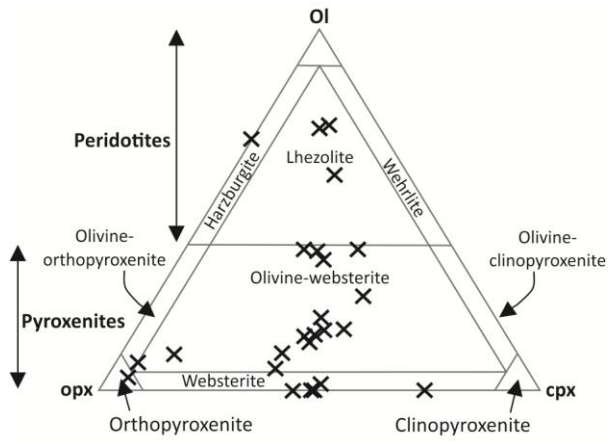(d) Leathaid Domain folds  (e) Leathaid Domain - north  (f) Leathaid Domain - south
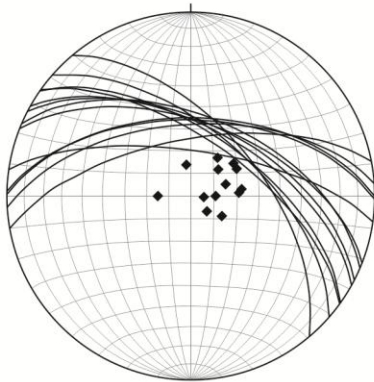
+ Laxfordian foliation (n=27)  ▲ TTG gneissosity (S1; n=216)  ○ Ben Strome Complex layering (n=90)  ＼ F2 axial planes (n=13)  ◆ F2 fold hinges (n=12)
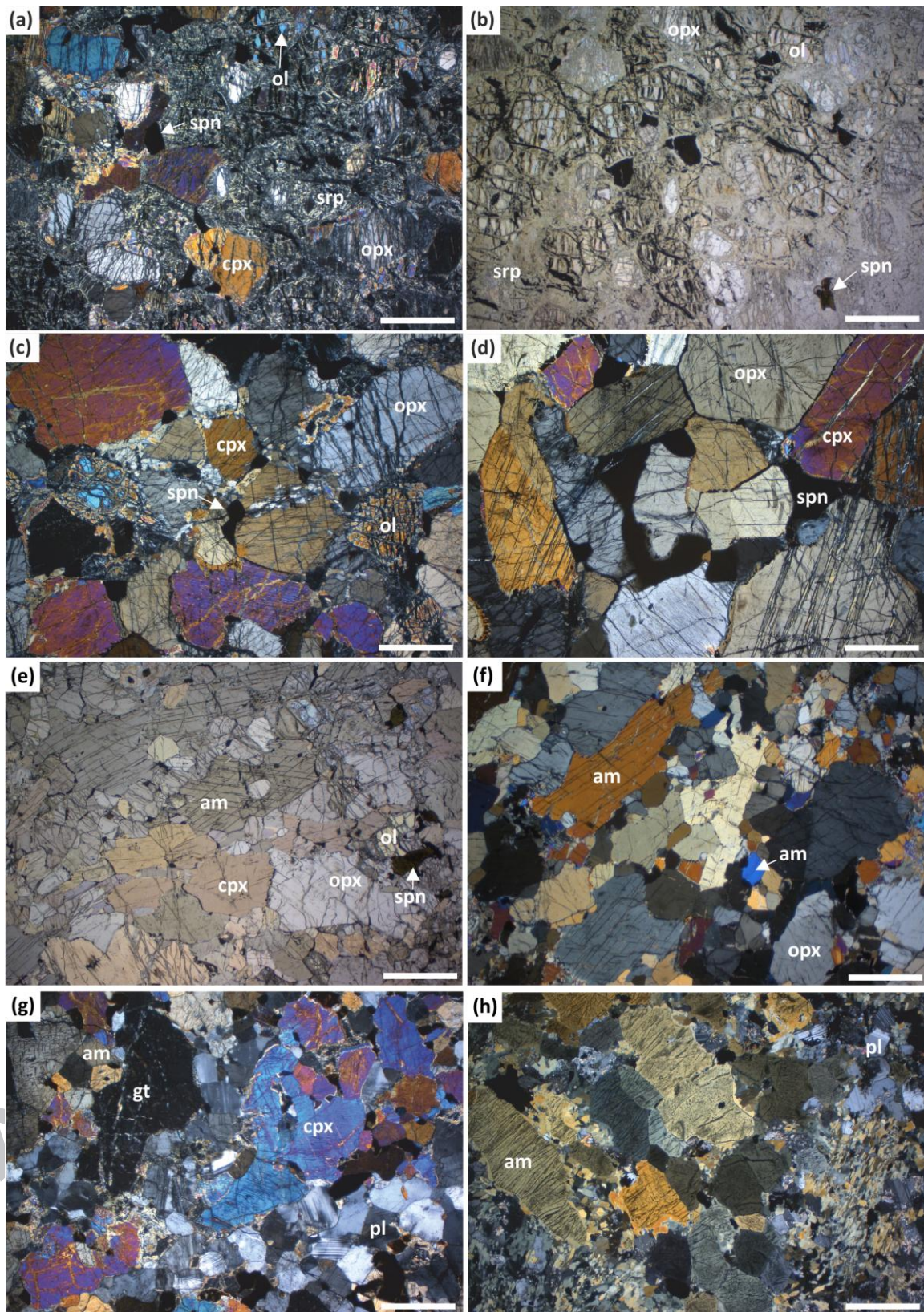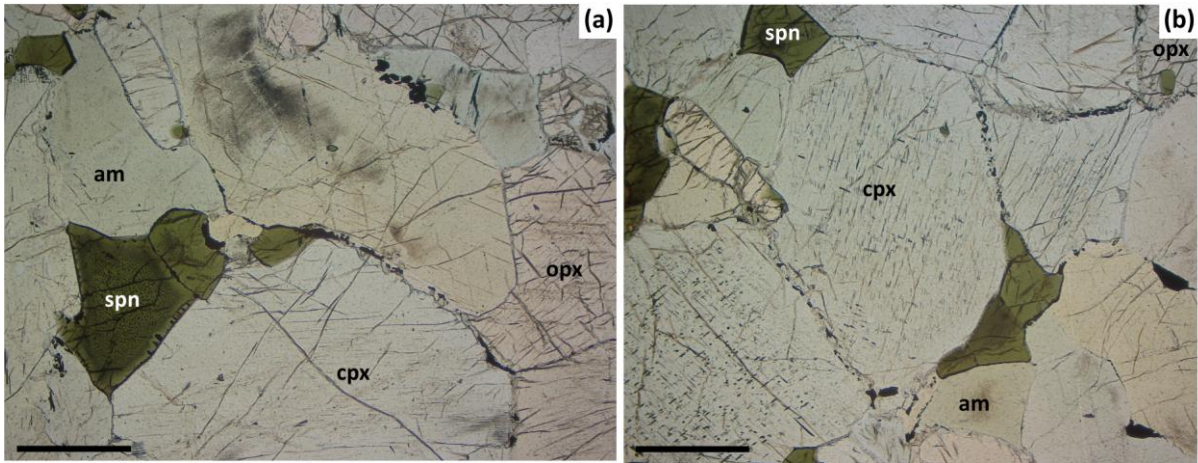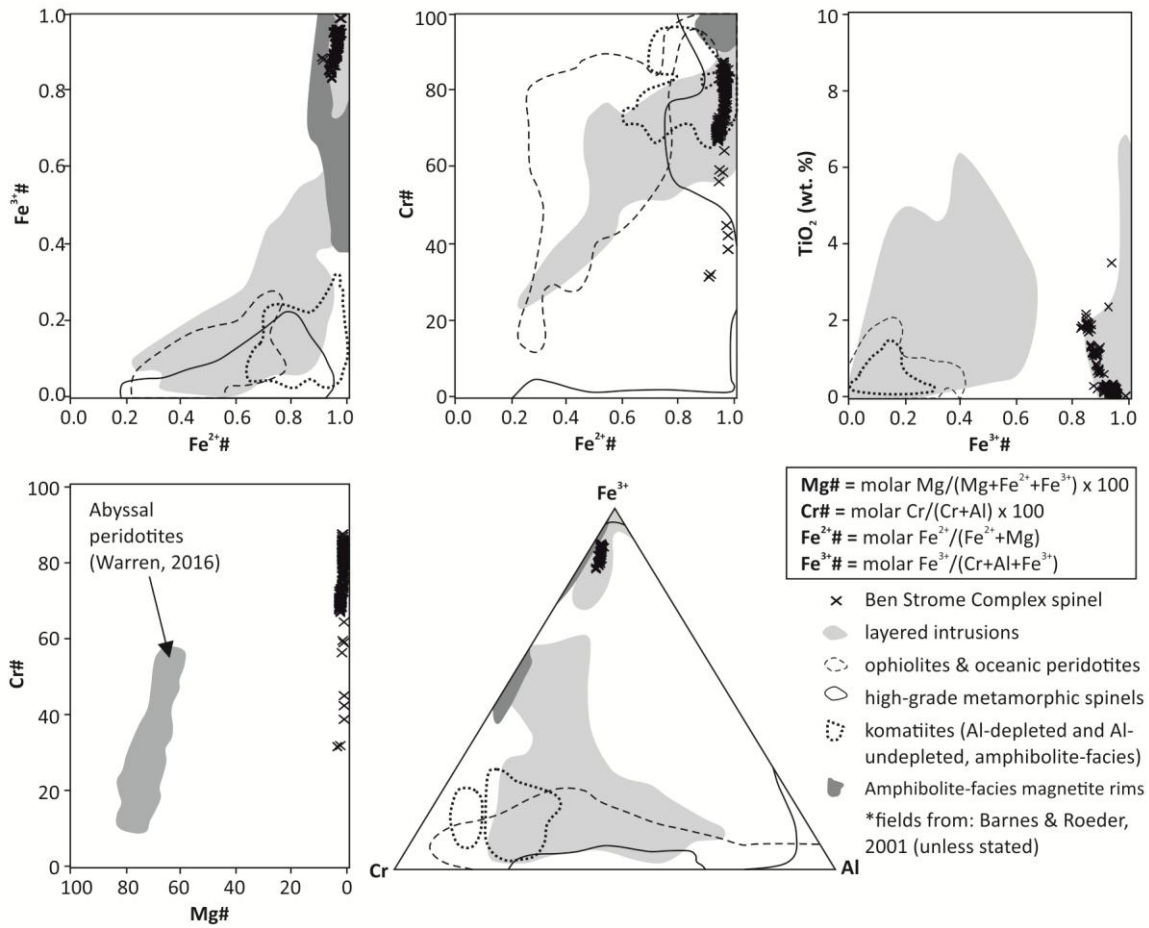
49

(a)

(b)

(c)

(d)

leucosome

**(a) this study**

apparent discordance of contact and layering is a function of topography

Line of transect detailed in (b)

A894

Badcall Bay

31
28
26
28
34   28
B
31   28
29
20   31
27
33   28
29
31
38   27   34   31
24   30   32
33
N
50 m

Geodh' nan Sgadan

**Legend - this study; (a) and (b)**

- scourie dyke
- quartz-feldspar pegmatite (felsic leucosome)
- trondhjemite sheet
- TTG gneiss
- mafic rocks (gabbro-dominated)
- fault
- contact (dashed=inferred)
- 26  gneissosity/layering measurement
- line of transect logged in (b)
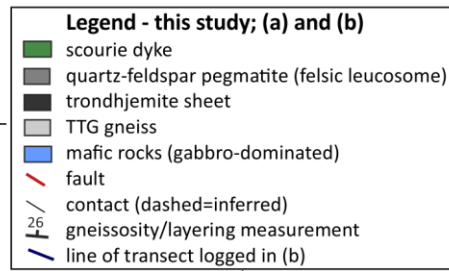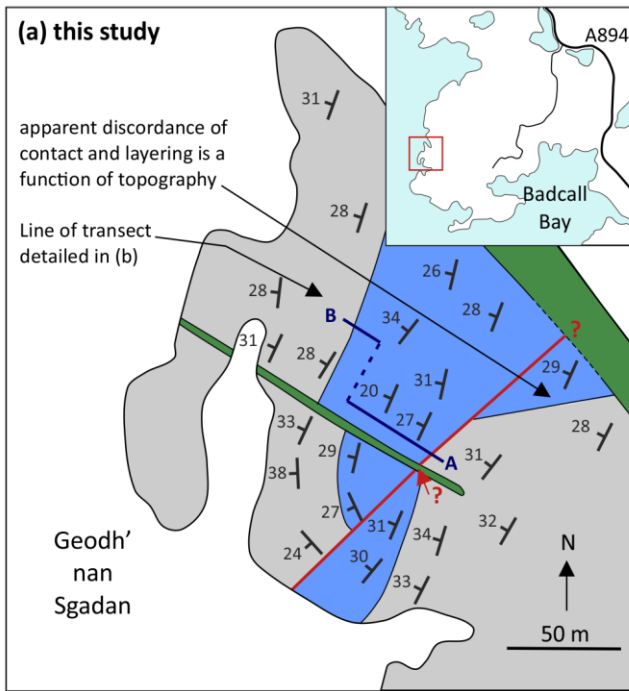
**(b) stratigraphic log (this study)**

B

17 m
16 m — Sharp contact
15 m — xxxx — 20 cm thick, garnet-rich horizon
14 m — Well-defined, mm-scale layering
13 m — Sheet of trondjemite varies in thickness along strike (80 cm - 160 cm)
12 m
11 m — Poorly-developed layering
10 m — Sharp contacts, with overlying mafic rocks veined by cm-scale quartz feldspar pegmatite
9 m — Rare cm-scale, cross-cutting, quartz-feldspar pegmatite
8 m — High density of cross-cutting quartz-feldspar pegmatite
7 m
6 m — Minimal truncation of mm-scale layering
5 m — Moderately-developed, mm to cm-scale layering shows truncation and is marked by more felsic layers
4 m
3 m — Faulted contact not exposed on line of transect
2 m
1 m
0 m

A

**(c) Rollinson & Windley, 1980**

N
shear zone
exposure obscured
50 m
30
35
26
32
34   36   80
26
38
40   36
36
36

proposed cross-cutting relationship

**Legend - Rollinson & Windley (1980) map; (c)**

- scourie dyke
- intrusive trondhjemite
- banded leucogneiss with ultramafic pods
- gabbro
- leuco-gabbro
- contact
- 26  gneissosity/layering measurement

55

**Legend:**
- Oceanic crust
- Greenstone belt
- TTG
- Archaean crust
- Layered intrusion (possible geotectonic environment for the Ben Strome Complex)

**SAGDUCTION MODEL (1)**

**SUBDUCTION MODEL**

**(5)** **(4)** **(3)** **(2)**

**(6)** Invasion of ultramafic-mafic crust by TTG magmas (e.g. Sills, 1981)

**(1)** Sagduction model (e.g., Johnson et al., 2016): remnants of intracratonic greenstone belts that "sank" into the deep crust.
**(2)** Obducted remnants of oceanic crust (e.g., Park and Tarney, 1987).
**(3)** Subduction-related sill-like layered intrusion / magmatic underplating.
**(4)** Rift-related sill-like layered intrusion.
**(5)** Plume-related sill-like layered intrusion.

# Re-evaluating ambiguous age relationships in Archean cratons: implications for the origin of ultramafic-mafic complexes in the Lewisian Gneiss Complex

George L. Guice, Iain McDonald, Hannah S. R. Hughes, John M. MacDonald, Thomas G. Blenkinsop, Kathryn M. Goodenough, John W. Faithfull, Robert J. Gooday

Highlights:

- We re-evaluate relations between Archean mafic-ultramafic complexes and TTG gneiss.

- Layering and spinel geochemistry are both consistent with a layered intrusion origin.

- Ben Strome (and related complexes) represents a layered intrusion emplaced *into* TTG.

- The Lewisian records multiple phases of Archean mafic-ultramafic magmatism.

- Primary magmatic events are masked by subsequent high grade metamorphism.